Inorganic Chemistry

Article

pubs.acs.org/IC

Role of Fe(IV)-Oxo Intermediates in Stoichiometric and Catalytic Oxidations Mediated by Iron Pyridine-Azamacrocycles

Wanhua Ye,[†] Douglas M. Ho,[‡] Simone Friedle,[§] Taryn D. Palluccio,[†] and Elena V. Rybak-Akimova*[,†]

[†]Department of Chemistry, Tufts University, Medford, Massachusetts 02155, United States

[‡]Department of Chemistry and Chemical Biology, Harvard University, Cambridge, Massachusetts 02138, United States

[§]Department of Chemistry, Massachusetts Institute of Technology, Cambridge, Massachusetts 02139, United States

Supporting Information

ABSTRACT: An iron(II) complex with a pyridine-containing 14-membered macrocyclic (PyMAC) ligand **L1** (**L1** = 2,7,12-trimethyl-3,7,11,17-tetra-azabicyclo[11.3.1]heptadeca-1(17),13,15-triene), **1**, was prepared and characterized. Complex **1** contains low-spin iron(II) in a pseudo-octahedral geometry as determined by X-ray crystallography. Magnetic susceptibility measurements (298 K, Evans method) and Mössbauer spectroscopy (90 K, δ = 0.50(2) mm/s, ΔE_Q = 0.78(2) mm/s) confirmed that the low-spin configuration of Fe(II) is retained in liquid and frozen acetonitrile solutions. Cyclic voltammetry revealed a reversible one-electron oxidation/reduction of the iron center in **1**, with $E_{1/2}(Fe^{III}/Fe^{II})$ = 0.49 V vs Fc^+/Fc, a value very similar to the half-wave potentials of related macrocyclic complexes. Complex **1** catalyzed the epoxidation of cyclooctene and other olefins with H_2O_2. Low-temperature stopped-flow kinetic studies demonstrated the formation of an iron(IV)-oxo intermediate in the reaction of **1** with H_2O_2 and concomitant partial ligand oxidation. A soluble iodine(V) oxidant, isopropyl 2-iodoxybenzoate, was found to be an excellent oxygen atom donor for generating Fe(IV)-oxo intermediates for additional spectroscopic (UV−vis in CH_3CN: λ_{max} = 705 nm, $\varepsilon \approx 240$ M^{-1} cm^{-1}; Mössbauer: δ = 0.03(2) mm/s, ΔE_Q = 2.00(2) mm/s) and kinetic studies. The electrophilic character of the $(\mathbf{L1})Fe^{IV}{=}O$ intermediate was established in rapid (k_2 = 26.5 M^{-1} s^{-1} for oxidation of PPh_3 at 0 °C), associative ($\Delta H^{\ddagger}$ = 53 kJ/mol, $\Delta S^{\ddagger}$ = −25 J/K mol) oxidation of substituted triarylphosphines (electron-donating substituents increased the reaction rate, with a negative value of Hammet's parameter ρ = −1.05). Similar double-mixing kinetic experiments demonstrated somewhat slower (k_2 = 0.17 M^{-1} s^{-1} at 0 °C), clean, second-order oxidation of cyclooctene into epoxide with preformed $(\mathbf{L1})Fe^{IV}{=}O$ that could be generated from $(L1)Fe^{II}$ and H_2O_2 or isopropyl 2-iodoxybenzoate. Independently determined rates of ferryl(IV) formation and its subsequent reaction with cyclooctene confirmed that the Fe(IV)-oxo species, $(\mathbf{L1})Fe^{IV}{=}O$, is a kinetically competent intermediate for cyclooctene epoxidation with H_2O_2 at room temperature. Partial ligand oxidation of $(\mathbf{L1})Fe^{IV}{=}O$ occurs over time in oxidative media, reducing the oxidizing ability of the ferryl species; the macrocyclic nature of the ligand is retained, resulting in ferryl(IV) complexes with Schiff base PyMACs. NH-groups of the PyMAC ligand assist the oxygen atom transfer from ferryl(IV) intermediates to olefin substrates.

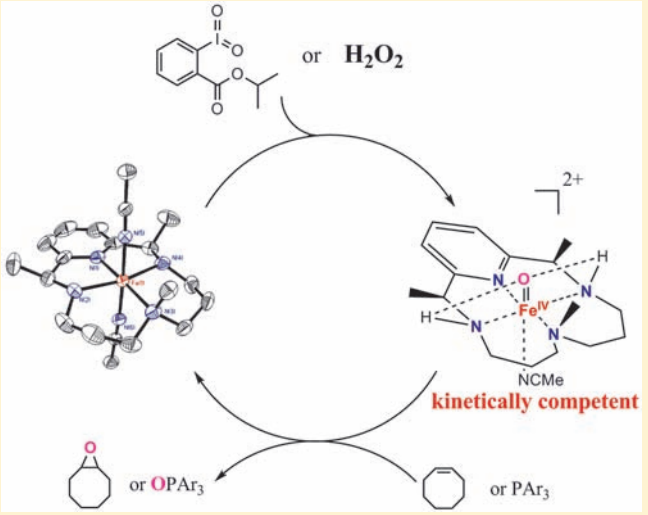

INTRODUCTION

Increasing interest in synthetic applications of cheap, readily available, nontoxic metals, such as iron, inspires the search for biomimetic oxidation catalysts.[1] Key mechanistic insight into biological and biomimetic oxidations is gained by identifying metal-based intermediates and characterizing their reactivity with target substrates. High-valent iron-oxo intermediates, such as $(P^{\cdot-})Fe^{IV}{=}O$, are well-established active oxidants in heme chemistry.[2,3] Similarly, dinuclear nonheme iron enzymes, such as methane monooxygenase, rely on the potent oxidizing ability of high-valent diiron(IV) intermediates that are competent to oxidize hydrocarbons.[4−11] Recent developments in mononuclear nonheme iron chemistry[10−15] demonstrate the importance of $Fe^{IV}{=}O$ intermediates in the catalytic cycles of a number of enzymes, including pterin-dependent phenylalanine hydroxylase and α-ketoglutarate-dependent prolyl hydroxylase.[4,5,16,17] Several high-spin Fe(IV) intermediates in mononuclear nonheme iron enzymes were spectroscopically characterized and in certain cases were shown to be kinetically competent oxidants of the enzyme's biological targets.[5,16,18,19] Other examples of observable iron(IV) intermediates in

Received: November 13, 2011
Published: April 25, 2012

   dx.doi.org/10.1021/ic202435r | *Inorg. Chem.* 2012, 51, 5006−5021

biological systems include soybean lipoxygenase-3,[10] naphthalene dioxygenase,[20] and α-keto acid-dependent dioxygenase (TauD).[16,21]

Iron complexes with polyamine or aminopyridine ligands are frequently used as models of nitrogen-rich active sites of nonheme oxidases and oxygenases.[10,15,22,23] Similar to enzymes, several types of metal−oxygen intermediates were identified in reactions of these synthetic complexes with peroxides and other oxygen atom donors. Recently discovered iron(IV)-oxo species are of particular interest, with several of them crystallized at low temperature and structurally characterized.[24−26] Notably, the first crystallographically characterized ferryl(IV) complex contained a tetraazamacrocyclic (tetramethylcyclam) ligand,[27] and characterization of an Fe^{IV}=O complex supported by an acyclic aminopyridine ligand soon followed.[28] A number of related ferryl(IV) species were identified and characterized by spectroscopic methods;[24−26] polyamine azamacrocycles or acyclic aminoopyridine ligands were predominantly utilized in this chemistry (Figure 1). Examples of macrocyclic tetradentate

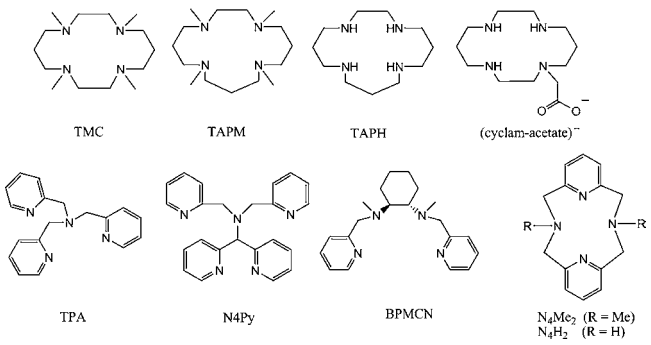

Figure 1. Selected tetra- and pentadentate ligands that support high-valent iron-oxo intermediates.

N4 systems that stabilize Fe(IV)-oxo intermediates include the oxoiron(IV) generated from iron(II) complexes with TMC (1,4,8,11-tetramethyl-1,4,8,11-tetraazacyclotetradecane),[27] TAPM (1,4,8,12-tetramethyl-1,4,8,12-tetraazacyclopentadecane),[29] and TAPH (1,4,8,12-tetraazacyclopentadecane).[29] Wieghardt et al. reported the generation of an oxoiron(IV) intermediate based on the cyclamacetate (1,4,8,11-tetraazacyclotetradecane 1-acetate) macrocycle.[30] Iron(IV)-oxo intermediates were also characterized in systems containing polydentate aminopyridine ligands such as TPA (tris(2-pyridinemethyl)amine,[28] N4Py (*N*,*N*-bis(2-pyridylmethyl)-*N*-bis(2-pyridyl)methylamine),[31] and BPMCN (*N*,*N*-bis(2-pyridylmethyl)-*N*,*N*-dimethyl-*trans*-1,2-diaminocyclohexane).[32] These oxoiron(IV) species can be generated by using single oxygen atom donors such as iodosylbenzene (PhIO),[29,31,33−36] *m*-chloroperoxybenzoic acid (*m*-CPBA),[37,38] peracetic acid (CH_3COOOH),[28,34] potassium monopersulfate ($KHSO_5$),[34] NaOX (X = Cl or Br)[39] or O_3.[30,40]

Advances in our understanding of the mechanistic role of Fe(IV)-oxo intermediates in nonheme iron enzymes and synthetic accessibility of similar iron(IV) intermediates in model complexes have prompted investigators to view high-valent iron(IV)-oxo species as key intermediates responsible for oxygen atom transfer to organic substrates in catalytic oxidations.[6−8,12,13,26,41−52] However, direct experiments that characterize the reactivity of iron(IV) intermediates are limited and include primarily stoichiometric reactions.[24,53] Pregenerated ferryl(IV) species can participate in oxygen atom transfer reactions with phosphines, sulfides, and certain olefins (e.g., cyclooctene),[49,54−57] in hydrogen atom abstractions (e.g., formation of anthracene from dehydroanthracene),[46,50,58,59] and in electron transfer reactions.[60,61] However, questions about the intermediacy of ferryl(IV) in catalytic oxidations with nonheme iron complexes remain.[13,56,57,62,63] For example,

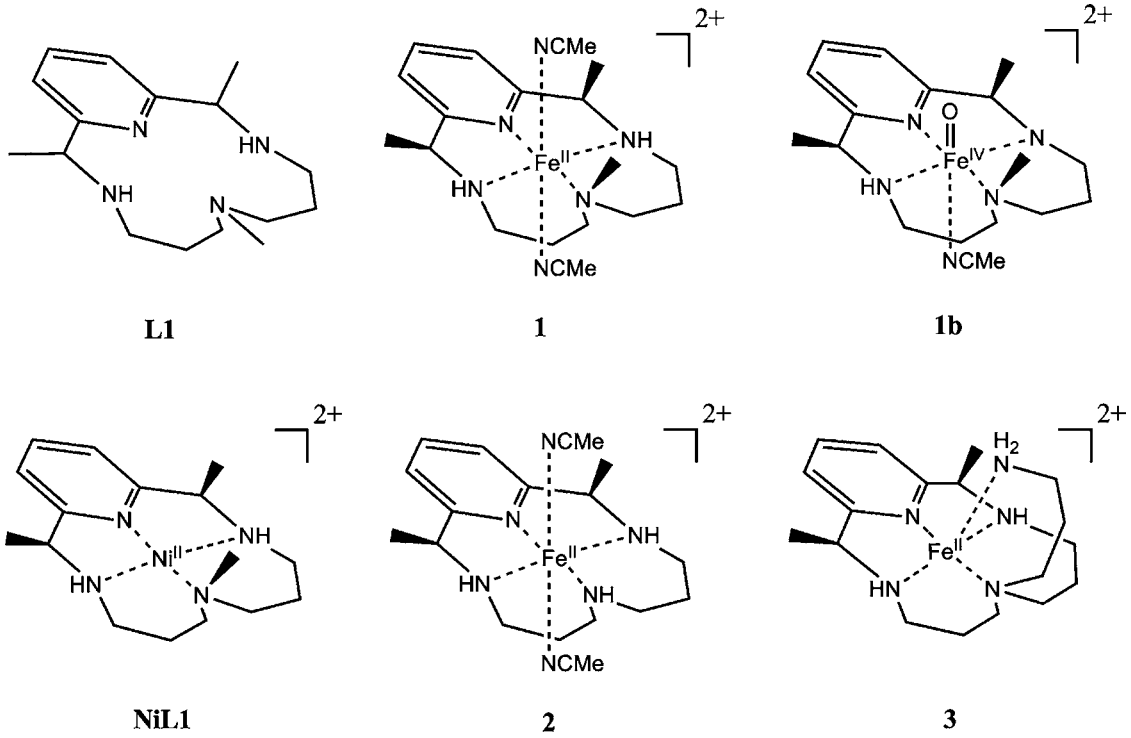

Figure 2. Pyridine-containing macrocycles (PyMACs) used in this work.

dx.doi.org/10.1021/ic202435r | *Inorg. Chem.* 2012, 51, 5006−5021

efficient olefin epoxidation with hydrogen peroxide catalyzed by $Fe(TPA)^{2+}$ or $Fe(BPMEN)^{2+}$ in the presence of acetic acid proceeds under conditions that favor the formation of $(L)Fe^{IV}{=}O$. This intermediate was independently generated and subjected to reactions with olefins. Surprisingly, no epoxide (or an alternative product, *cis*-diol) formed in these experiments, clearly demonstrating that ferryl(IV) is not a competent intermediate in these epoxidations or related dihydroxylations.[56] Given that epoxidation is a synthetically useful and mechanistically important process,[64] further studies are clearly needed to understand oxygen atom transfer in catalytic reactions with synthetic nonheme iron complexes. Using hydrogen peroxide, a nontoxic oxidant that generates water as the oxidation byproduct, is particularly attractive.[54−57]

In the present work, we set out to explore the reactivity of Fe(IV) intermediates derived from biomimetic iron complexes that are catalytically active in olefin epoxidation with H_2O_2. Our group is interested in using pyridine-macrocycle ligands (PyMACs), depicted in Figure 2, to explore the reactivity of the iron complexes in catalytic oxidations. These ligands combine the advantages of macrocyclic polyamines, which prevent iron loss under catalytic conditions by forming thermodynamically and kinetically stable iron complexes, and those of aminopyridine ligands that are capable of stabilizing a variety of iron-based intermediates. In our previous study,[65] we reported high activity of the iron(II) complex **3** in olefin epoxidation with H_2O_2 in the presence of HOTf. To focus on the role of iron(IV) intermediates in oxidations catalyzed by Fe(PyMAC) complexes, we now prepared a simpler structural analogue of **3**, an iron(II) complex with a pyridine-containing 14-membered macrocyclic ligand **L1** (**L1** = 2,7,12-trimethyl-3,7,11,17-tetra-azabicyclo[11.3.1]heptadeca-1(17),13,15-triene). This unfunctionalized complex, **1**, generates an iron(IV)-oxo intermediate (**1b**) using isopropyl 2-iodoxybenzoate as an oxidant. Spectroscopic characterization of **1b** and its reactivity with substrates (olefins or triarylphosphines) under stoichiometric and catalytic conditions are reported.

EXPERIMENTAL SECTION

General Considerations. All reagents were obtained from commercially available sources and used as received unless otherwise noted. All manipulations of air-sensitive materials were carried out in an MBraun glovebox under an atmosphere of ultra high purity argon. Isopropyl 2-iodoxybenzoate was synthesized following a published procedure.[66] $H_2{}^{18}O_2$ (90% ^{18}O-enriched, 2% solution in $H_2{}^{16}O$) and $H_2{}^{18}O$ (98% ^{18}O-enriched) were purchased from Cambridge Isotope Laboratories Inc. $Fe(OTf)_2{\cdot}2CH_3CN$ (OTf = $CF_3SO_3^-$) was prepared from $FeCl_2$ and $CF_3SO_3SiMe_3$ in CH_3CN following an unpublished procedure provided by Dr. Miquel Costas and Prof. Lawrence Que, Jr. $^{57}Fe(OTf)_2{\cdot}2CH_3CN$ (ca. 40% ^{57}Fe with respect to total iron content) was prepared by a literature procedure from elemental iron.[67] The olefin substrates were purified by passing through a short column of activated alumina and stored in a glovebox. All concentrations intended for the stopped-flow experiments are reported before mixing unless otherwise noted.

Physical Methods. Room temperature UV−vis spectra were recorded on a Jasco V-570 spectrophotometer. Electrospray ionization-mass spectrometry (ESI-MS) was performed on a Thermo Finnigan LCQ quadrupole field mass spectrometer with electrospray ionization in the positive ion detection mode. NMR spectra were recorded in $CDCl_3$ at 300 K on a Bruker DPX 300 MHz spectrometer; chemical shifts in δ are reported versus tetramethylsilane. GC-MS analyses were performed using a Shimadzu QP5050A mass spectrometer connected to a Shimadzu GC-17A gas chromatograph equipped with Rtx-XLB column (length, 30 m; i.d. 0.25 mm; film thickness, 0.25 μm). Helium at a flow rate of 45 cm^3/s was used as the carrier gas. Injections were made in the splitless mode using an initial column temperature of 50 °C. The temperature was raised at 15 °C/min until 320 °C. Full scan was performed using ionization energy of 70 eV. Elemental analyses were performed by Schwarzkopf Microanalytical Laboratory, Inc. (Woodside, NY).

X-ray Crystallography. Single-crystal X-ray data for **NiL1** (see Supporting Information) and **1** were collected using a Bruker SMART APEXII diffractometer equipped with an Oxford Cryosystems 700 Series Cryostream Cooler and Mo Kα (λ = 0.71073 Å) radiation at 173 K. All structures were solved by direct methods using SHELXTL[68] and were refined against all reflections by full-matrix least-squares on F^2 using SHELXTL. Specific crystal, reflection, and refinement data for **1** are contained in Table 1. The macrocyclic cation in **NiL1** was located in the symmetry plane and suffered from whole molecule disorder along with disorder of the counterions; complex **1** contained only disordered triflate counterions (see Supporting Information for details).

Table 1. Crystallographic Data, Experimental Conditions, and Refinement Details for 1

crystal data	**1**
chemical formula	$C_{22}H_{34}F_6FeN_6O_6S_2$
Fw	712.52
crystal system	monoclinic
space group	$P2_1/c$
a (Å)	16.4722(6)
b (Å)	14.1244(5)
c (Å)	13.3141(5)
β (deg)	100.968(3)
volume (Å^3)	3050.21(19)
Z	4
D_c (g cm^{-3})	1.552
crystal size (mm^3)	0.20 × 0.10 × 0.04
abs coeff (mm^{-1})	0.715
transmission range	0.9754−0.8703
no. reflns collected	19365
no. indep collected	5365
R_1 [$I > 2\sigma(I)$][a]	0.0619
wR_2[b] (all data)	0.1317
GOF (F^2)	1.020
diff peaks (e Å^{-3})	0.537, −0.280

[a] $R_1 = \sum||F_o| - |F_c||/\sum|F_o|$. [b] $wR_2 = \{\sum[w(F_o^2 - F_c^2)^2]\}^{1/2}$ where $w = 1/\sigma^2(F_o^2) + (aP)^2 + bP$; R factors based on F^2 are statistically about twice as large as those based on *F*.

^{57}Fe Mössbauer Spectroscopy. Mössbauer spectra were recorded on an MS1 spectrometer (WEB Research Co.) with a ^{57}Co source in an Rh matrix maintained at room temperature. CH_3CN was used as solvent for the preparation of all samples. A number of separate samples of the intermediate and decomposition products were prepared and measured to confirm reproducibility. ^{57}Fe-enriched samples of the reaction intermediate were prepared with $^{57}Fe(OTf)_2{\cdot}2CH_3CN$. In general, a solution of isopropyl 2-iodoxybenzoate (20 mg, 0.5 mL) was added to a solution of **1** (4.5 mg, 0.35 mL) in CH_3CN at −40 °C. After a short period of time (seconds), the reaction mixture was transferred to a precooled nylon sample holder (−40 °C) and quickly frozen in liquid nitrogen. Data were acquired at 90 K without any applied magnetic fields. Mössbauer spectra were fit to Lorentzian lines by using the WMOSS plot and fit software.[69] The isomer shift (δ) values are quoted relative to natural iron foil used for velocity calibration at 298 K.

Cyclic Voltammetry. Cyclic voltammetry was carried out using a CH Instruments electrochemical analysis system (Model 830) using a conventional three-electrode configuration. A glassy carbon electrode

dx.doi.org/10.1021/ic202435r | Inorg. Chem. 2012, 51, 5006−5021

Scheme 1. Synthesis of Iron(II) Complex 1

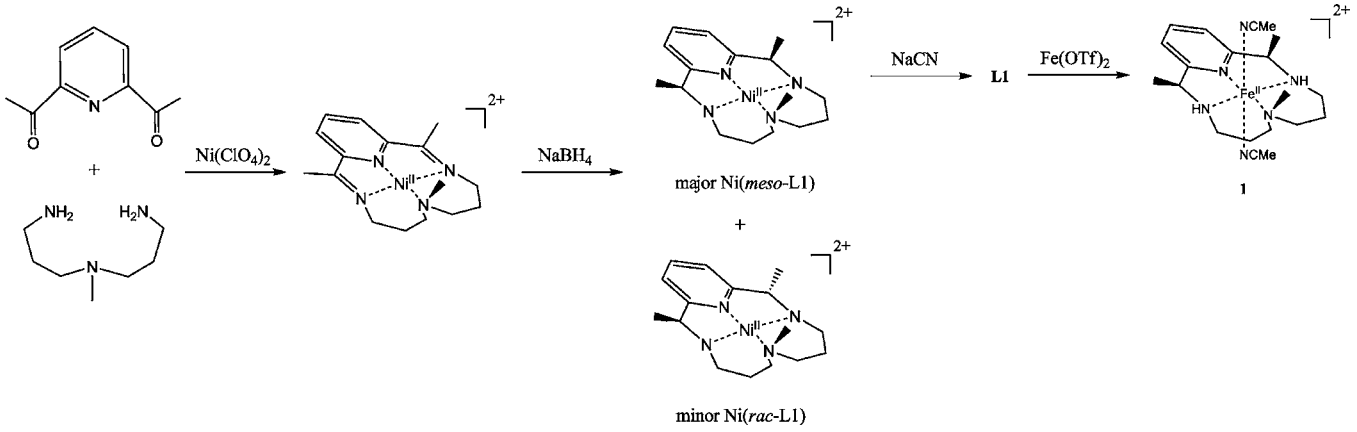

(3 mm diameter) was used as the working electrode and platinum wires as counter and reference electrodes. Measurements were performed with 2 mM analyte in CH_3CN at ambient temperature under argon using 0.1 M tetra-*n*-butylammonium hexafluorophosphate as the supporting electrolyte. The range of potentials was scanned at a rate of 100 mV s^{-1}. The ferrocene/ferrocenium (Fc/Fc^+) reference couple was used as an internal standard.

Measurements of Effective Magnetic Moment in Solutions. Measurements by Evans method were performed on a Bruker DPX-300 spectrometer at 25 °C.[70−72] A solution of complex **1** (1 mM) in 0.5 mL of CD_3CN (with 1% tetramethylsilane, TMS) was prepared under an argon atmosphere. The effective magnetic moment (μ_{eff}) was calculated from $\mu_{eff} = 8\chi_g M_w T$, where χ_g ($cm_3\ g^{-1}$) is the corrected molar susceptibility derived from $\chi_g = 3\delta\nu/4\pi\nu_o C M_w + \chi_o$.[73] $\delta\nu$ is the shift in frequency (Hz) from the value found for the pure solvent, C is the concentration of the complex (mol cm^{-3}), M_w is the molecular weight of the complex (g mol^{-1}), ν_o is the operating frequency of the NMR spectrometer (Hz), and χ_o is the mass susceptibility of the pure solvent (-0.682×10^{-6} $cm^3\ g^{-1}$ for acetonitrile). The $4\pi/3$ shape factor is for a cylindrical sample in a superconducting magnet. The number of unpaired electrons per molecule, n, can then be easily derived from the magnetic moment using $\mu^2 = g^2 S(S+1)$, where S is the electronic spin and g the Landé factor. This can be further simplified into $n(n+2)$ for $g = 2$.[74]

Catalysis Experiments. A solution of complex **1** was prepared in a glovebox under an argon atmosphere (0.8 μmol, 5 mol % catalyst with respect to olefin substrate) in 1.0 mL of dry CH_3CN. *cis*-Cyclooctene or 1-decene (25 μL, 0.016 mmol) was added to the catalyst solution via syringe. To this mixture was added H_2O_2 (30 μL, 0.024 mmol) all at once. The reaction was run anaerobically at room temperature for 5 min followed by GC-MS. The molar ratio of catalyst/substrate/H_2O_2 is 1/20/30. In the ^{18}O-labeling experiments, $H_2{}^{18}O_2$ or $H_2{}^{18}O$ (300 μL, 0.24 mmol, 0.8 M) was added to the catalyst solution following the method described as above.

Stopped-Flow Kinetic Experiments. Stopped-flow spectrophotometry was performed on a TgK Scientific (formerly, Hi-Tech Scientific, U.K.) SF-61DX2 cryogenic double-mixing stopped-flow system[75] equipped with a J&M TIDAS diode array spectrophotometer (MCS UVNIR 500-3, 200−1024 nm).[76] Low temperatures were maintained through the use of a liquid-nitrogen-cooled ethanol bath equipped with a temperature controller. All flow lines of the instrument were extensively washed with oxygen-free, argon-saturated anhydrous CH_3CN before charging the driving syringes with reactant solutions. CH_3CN solutions of the reagents were prepared in a glovebox filled with argon and placed in Hamilton gastight syringes. Kinetic Studio[77] and J&M TIDAS software packages were used to control the instrument and collect data. The raw kinetic data were treated with Kinetic Studio software from TgK Scientific, and with Spectfit/32 Global Analysis System software from Spectrum Software Associates.[78]

Synthesis of $[Ni^{II}(L1)](ClO_4)_2$ (NiL1). **NiL1** and ligand **L1** were prepared following a literature procedure,[79,80] except that the amine 1,7-diamino-4-methyl-4-azaheptane was used. Recrystallizing the product from warm (65 °C) water allowed for separation of isomers. The first deep orange crystalline complex contains mostly *meso* ligand; the latter orange complex contains mostly *rac* ligand. ESI(+)−MS (CH_3CN) m/z: $[Ni(L1)]^{2+}$ calcd for 165.1; Found, 165.2; $\{[Ni(L1)]-H\}^+$ calcd for 329.2; Found, 329.4; $\{[Ni(L1)](ClO_4)\}^+$ calcd for 429.1; Found, 429.2. Stereochemistry of $Ni(L1)(ClO_4)_2$ was confirmed by X-ray crystallography (Supporting Information).

Synthesis of Ligand L1. A solution of **NiL1** (0.05 g, 0.094 mmol) in 5 mL of warm water, and sodium cyanide (0.028 g, 0.564 mmol) was added. The solution changes color immediately, proceeding from red-orange, through violet to yellow. After stirring for 10 min, the solution was extracted with dichloromethane (3 × 15 mL); the combined extracts were dried with anhydrous $MgSO_4$ and the dichloromethane was removed on a rotary evaporator to leave the product as yellow oil. ESI(+)−MS (CH_3CN) m/z: $(L1+H)^+$ calcd for 276.2; Found, 276.5. ^1H NMR of a pure *meso* **L1** (δ, ppm in $CDCl_3$): 1.41 (6H, d), 1.64−1.69 (4H, m), 1.97−2.56 (8H, m), 3.10 (4H, s), 3.63 (2H, quartet), 6.93 (2H, d), 7.48 (1H, t). ^1H NMR of a pure *rac* **L1** (δ, ppm in $CDCl_3$): 1.41 (6H, d), 1.64−1.69 (4H, m), 1.97−2.56 (8H, m), 3.10 (4H, s), 3.79 (2H, quartet), 7.05 (2H, d), 7.58 (1H, t). Oxidative degradation of this material in boiling aqueous HNO_3/$Na_2S_2O_8$, followed by neutralization and addition of excess dimethylglyoxime did not afford red $Ni(dmg)_2$ product, indicating essentially quantitative removal of nickel from **NiL1**.

Synthesis of $[Fe^{II}(L1)(OTf)_2](CH_3CN)_2$ (1). $Fe(OTf)_2{\cdot}2CH_3CN$ (0.014 g, 0.033 mmol) dissolved in 3 mL of dry CH_3CN was added to a solution of **L1** (0.01 g, 0.036 mmol) in 3 mL of dry CH_3CN under an argon atmosphere. Upon mixing, the solution turned red. Dark-red crystals were obtained after 4−5 days by vapor diffusion of diethyl ether into this solution. Yield: 0.0156 g (65%). ESI(+)−MS (CH_3CN) m/z: $\{[Fe(L1)](OTf)\}^+$ calcd for 481.1; Found, 481.2. Anal. Calcd for $C_{22}H_{34}N_6FeO_6F_6S_2$: C, 37.09; H, 4.81; N, 11.79; Fe, 7.84. Found: C, 37.15; H, 5.26; N, 11.76; Fe, 7.87. The preparation of $[^{57}Fe(L1)(OTf)_2]^{2+}$**1** was conducted in an analogous manner by using $^{57}Fe(OTf)_2{\cdot}2CH_3CN$.

RESULTS AND DISCUSSION

Iron complexes with pyridine-containing macrocycles (PyMACs) displayed notable catalytic activity in catalytic oxidations with H_2O_2.[54,65] To focus on the reactivity of the unfunctionalized iron complex that is most closely related to catalytically active complexes **2** and **3** (Figure 2), we present here the synthesis and reactivity of **1**. Methylation of one nitrogen atom of the ring was expected to suppress oxidation and hydrolysis of the ligand in the most vulnerable aliphatic fragment. NH-groups adjacent to the pyridine ring were

dx.doi.org/10.1021/ic202435r | Inorg. Chem. 2012, 51, 5006−5021

retained because their presence did not suppress the catalytic activity of the functionalized PyMACs.[65] The relatively simple structure of the macrocycle allowed us to generate and characterize high-valent iron intermediates in reactions of **1** with oxidants. The reactions of transient iron(IV) intermediates with substrates (substituted triaryl phosphines or olefins) were studied by the stopped-flow technique, providing insight into the nature of reactive species in catalytic oxidations with H_2O_2.

Synthesis and Characterization of 1. Similarly to previously reported syntheses of Fe(PyMAC)'s,[65,79] the macrocycle was assembled on a nickel(II) template, using 2,6-diacetylpyridine as the dicarbonyl component and 1,7-diamino-4-methyl-4-azaheptane as the diamine component in the *Schiff* base condensation (Scheme 1). Incorporation of iron(II) required subsequent transmetalation. Transmetalation of the *Schiff* base nickel(II) complex did not produce satisfactory results because of the hydrolytic instability of the free *Schiff* base ligand. Instead, C═N double bonds in the Ni(II) *Schiff* base complex were reduced with $NaBH_4$, producing a mixture of *meso*- and *rac*-diastereomers that were separated by recrystallization. The structure of the major product, [Ni(*meso*-**L1**)]$(ClO_4)_2$, was confirmed by crystallography (Supporting Information, Figure S1). Demetalation of this complex afforded pure aminopyridine macrocycle ligand, *meso*-**L1**. The iron(II) complex was prepared from the appropriate iron(II) salt and the free ligand under anaerobic conditions, and was characterized by elemental analysis, electrospray mass spectrometry, IR, UV−vis, and single-crystal X-ray diffraction.

X-ray crystallographic analysis of complex **1** showed that the iron(II) ion is in an octahedral environment, defined by the four nitrogen atoms from **L1** and two coordinated acetonitrile molecules in the axial positions (Figure 3). Selected bond lengths and angles are listed in Table 2. The two methyl groups on the ligand are on the same side of the tetradentate macrocycle, as expected for the *meso* isomer identified in the nickel(II) precursor, **NiL1** (Supporting Information, Figure S2, Table S1). For **1**, the values of the N1−Fe1−N3 angle 177.61(15)° and N2−Fe1−N4 angle 166.96(18)° are observed. This geometry with a tetradentate macrocycle has also been found in nickel and iron analogues.[65,81−84] The Fe−N bond lengths in **1** range from 1.873(4) to 2.2(4) Å with the shortest bond length to the pyridine nitrogen 1.873(4) Å. The Fe−N separation is similar to those of a reported low-spin iron(II) complex (2.06−2.18 Å).[65,83]

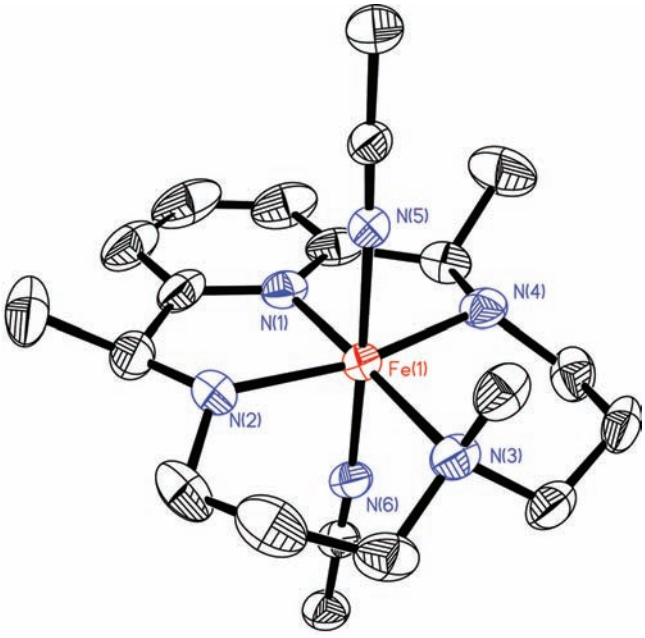

Figure 3. ORTEP diagram of the complex cation of **1** with thermal ellipsoids at 40% probability. Hydrogen atoms are omitted for clarity.

Table 2. Selected Bond Lengths (Å) and Angles (deg) for 1

	1
Fe(1)−N(1)	1.873(4)
Fe(1)−N(2)	1.996(4)
Fe(1)−N(3)	2.091(4)
Fe(1)−N(4)	2.2004(4)
Fe(1)−N(5)	1.937(4)
Fe(1)−N(6)	1.922(4)
N(1)−Fe(1)−N(2)	82.89(19)
N(1)−Fe(1)−N(3)	177.61(15)
N(1)−Fe(1)−N(4)	84.55(19)
N(1)−Fe(1)−N(5)	88.78(16)
N(1)−Fe(1)−N(6)	87.51(16)
N(2)−Fe(1)−N(3)	96.48(18)
N(2)−Fe(1)−N(4)	166.96(18)
N(2)−Fe(1)−N(5)	88.50(17)
N(2)−Fe(1)−N(6)	91.39(18)
N(3)−Fe(1)−N(4)	96.21(17)
N(3)−Fe(1)−N(5)	93.51(16)
N(3)−Fe(1)−N(6)	90.20(16)
N(4)−Fe(1)−N(5)	87.75(16)
N(4)−Fe(1)−N(6)	91.55(16)
N(5)−Fe(1)−N(6)	176.27(17)

Magnetic susceptibility measurements using Evans method were performed on **1** in CD_3CN. The peak of the standard, TMS, did not shift in the presence of **1** (no splitting of the TMS peak was observed for the sample containing a capillary with pure TMS/CD_3CN inserted in the CD_3CN solution of **1**), indicating the effective magnetic moment μ_{eff} = 0 T J^{-1}. Therefore, the low-spin configuration of iron(II) in crystalline **1** is retained in acetonitrile solutions.[85]

The Mössbauer spectrum of a frozen acetonitrile solution of **1** (90 K, zero field) confirmed this conclusion. The spectrum consisted of a sharp (Γ = 0.29 mm/s) quadrupole doublet with an isomer shift of δ = 0.50(2) mm/s and a quadrupole splitting parameter of ΔE_Q = 0.78(2) mm/s (Supporting Information, Figure S3), indicating a low-spin iron(II) complex. Mössbauer parameters of **1** are comparable to the parameters found in other low-spin ferrous complexes with macrocyclic ligands.[86−88]

A related iron(II) complex with a tetradentate aminopyridine macrocycle, **2** (Figure 2), was also previously shown to preferentially exist in a low-spin iron(II) form (μ_{eff} = 0 T J^{-1}) in acetonitrile solution, whereas **3**, which contains a pentadentate macrocycle, displayed an effective magnetic moment of μ_{eff} = 5.2 T J^{-1}, characteristic of iron(II) in a high-spin configuration.[65] It can be concluded that the denticity of PyMAC ligands allows for a high degree of control over the spin state of iron(II) in these complexes.

Close similarity in geometric and electronic structures between complex **1** and other low-spin Fe(II)-PyMACs suggested that their redox properties would likely be similar as well. Electrochemical experiments support this assumption,

dx.doi.org/10.1021/ic202435r | *Inorg. Chem.* 2012, 51, 5006−5021

revealing a reversible Fe^{3+}/Fe^{2+} redox wave in the cyclic voltammogram of **1**, with $E_{1/2}$ = 0.49 V (ΔE_p = 55 mV) vs Fc^+/Fc (Figure 4), a value very similar to previously measured half-

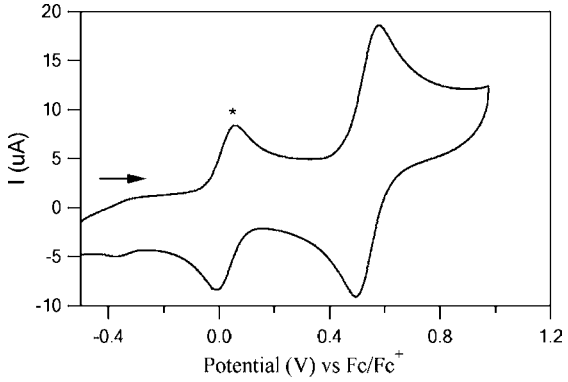

Figure 4. Cyclic voltammogram of complex **1** (2 mM in CH_3CN with 0.1 M [n-Bu_4N][PF_6] as the supporting electrolyte, under an argon atmosphere; scan rate 100 mV s^{-1}) . * Represents the Fc^+/Fc couple; a minor peak at −0.3 V is due to the impurity in the solvent system.

wave potentials for **2** and (**3**−H^+) (0.40 and 0.51 V, respectively).[65] Complex **1**, featuring a simple macrocyclic platform partially protected from oxidative decomposition by a methyl substituent on the middle nitrogen atom, is therefore a promising starting material for generating metal-based oxidizing intermediates. With the long-term goal of identifying catalytically important intermediates in mind, we explored the reactivity of new Fe(IV) intermediates generated from **1**. As a prerequisite for these studies, catalytic activity of **1** was examined first, followed by detailed investigations of the individual steps related to catalysis.

Catalytic Olefin Epoxidation. Catalytic activity of **1** was tested in olefin epoxidations with H_2O_2, a reaction catalyzed by structurally related Fe-PyMAC's **2** and **3**. Epoxidation of cyclooctene or 1-decene with H_2O_2 was studied under mild conditions identical to those used previously with **2** and **3** (Figure 2).[65] *cis*-Cyclooctene is commonly used as a substrate for catalyst screening in epoxidations with H_2O_2 in the presence of nonheme iron catalysts.[74] Terminal olefins, such as 1-decene, are more challenging substrates that only undergo epoxidation in the presence of highly reactive catalysts.[54] Table 3 shows epoxide yields and turnover numbers (TON) after 5 min of reaction, carried out under an argon atmosphere at room temperature.

Complex **1** was shown to catalyze epoxidation of both 1-decene and cyclooctene after 5 min of reaction, carried out under argon atmosphere at room temperature. Although epoxide yields and turnover numbers (18%, TON = 4 for 1-decene, and 36%, TON = 8 for cyclooctene, Table 3) are relatively low, the reaction is clearly catalytic. Longer reaction times did not increase the product yields, suggesting that epoxidation of olefins with H_2O_2 in the presence of **1** is rapid. The reaction exhibited high selectivity (80%) with respect to epoxides; other identified side products included *cis*-diol (ca. 0.5% with respect to 1-decene; ca. 0.7% with respect to cyclooctene) and traces of allylic alcohol (ca. 0.4%).

Catalytic activity of **1** in olefin epoxidations can be compared to the reactivity of analogous, previously studied PyMAC complexes **2** and **3** (Table 3). Complexes with tetradentate macrocycles, **1** and **2**, were catalytically active. Both complexes contained low-spin Fe(II) in a distorted octahedral geometry with two labile acetonitrile molecules occupying axial positions. **2** has shown a somewhat higher reactivity than **1** in both epoxidations, suggesting a possible involvement of the NH groups of the ligands in hydrogen peroxide activation. Complex **3**, which contains high-spin Fe(II) in a square-pyramidal geometry, turned out to be the least efficient catalyst among these three PyMACs. It should be noted, however, that protonation of the aminopropyl arm in **3** with externally added mineral acid dramatically improved its catalytic activity.[65] Although catalytic activity of **1** was relatively low, we did not attempt to optimize it in the current work. By analogy with previous studies of the other iron PyMACs, **2** and **3**, addition of acid can be suggested as a promising approach to increasing olefin conversion and epoxide yield in these systems and will certainly be tested in future experiments. For the present mechanistic study, however, we chose to avoid additives. The observation of catalytic turnover in epoxidation of olefins with H_2O_2 in the presence of **1** justified the subsequent search for reactive intermediates in this system.

Isotope labeling experiments provided initial insight into the mechanism of catalytic epoxidation with H_2O_2/**1**. Nearly quantitative incorporation of ^{18}O into the epoxide product was observed when the reaction was carried out in the presence of $H_2{}^{18}O_2$. ^{16}O-epoxide was detected when the reaction was carried out in the presence of H_2O_2 and $H_2{}^{18}O$. These

Table 3. Olefin Epoxidation Reaction with H_2O_2 Catalyzed by 1 and Related PyMAC Complexes

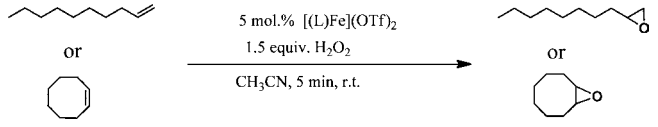

catalyst	olefin	epoxide[a] (%)	TON[b]	convn[c] (%)	selectivity[d] (%)	ref
1a	1-decene	18	4	22	81	this work
1a	cyclooctene	36	8	42	85	this work
1a	*cis*-2-heptene[f]	33	7.2	64	52	this work
2a[e]	1-decene	33 (20)	8 (4)	44(33)	75 (61)	this work[65]
2a[e]	cyclooctene	62 (32)	12(6.4)	71(43)	87 (74)	this work[65]
3a	1-decene	4	0.8	14	29	65
3a	cyclooctene	6	1.2	10	60	65

[a]Yield of epoxide with the respect to olefin. [b]Moles of epoxide per mol of catalyst. [c]Internal standard used: nitrobenzene. [d]Selectivity = GC yield/conversion. [e]Catalyst (7.2 M):substrate (144 M):H_2O_2 (216 M) = 1:20:30. Values shown in parentheses are taken from ref 65. [f]Reaction was performed in the presence of 1 equiv of triflic acid; no *trans*-epoxide was detected (side products included 2- and 3-heptanones).

dx.doi.org/10.1021/ic202435r | Inorg. Chem. 2012, 51, 5006−5021

observations are consistent with a metal-based, H_2O_2-derived oxidant that slowly exchanges with water. The *cis*-diol side product, obtained from $H_2{}^{18}O_2$ experiments, contained about one ^{18}O atom per molecule. While low yield of *cis*-diol limited the accuracy of isotope labeling studies, it appears that some oxygen in this product was derived from $H_2{}^{18}O_2$, and the remaining oxygen was incorporated from water. Control experiments demonstrated that the epoxide did not undergo hydrolysis under our typical epoxidation conditions. Although our isotope labeling results are limited, they agree with previously published extensive studies of analogous systems, which were interpreted as evidence for interconverting oxo-*bis*-hydroxo-forms of a high-valent metal-based oxidant.[25,89,90] Subsequent experiments were designed to observe metal-based intermediates in reactions of **1** with hydrogen peroxide or other oxidants.

Reactions of 1 with Oxidants and Formation of Iron(IV) Intermediates. *(a). Reaction with Hydrogen Peroxide.* In an attempt to identify transient, metal-based intermediates in the system containing **1** and hydrogen peroxide, stopped-flow experiments with spectrophotometric registration were performed, revealing a rapid reaction that occurs within seconds at 0 °C (Figure 5). During this time, a

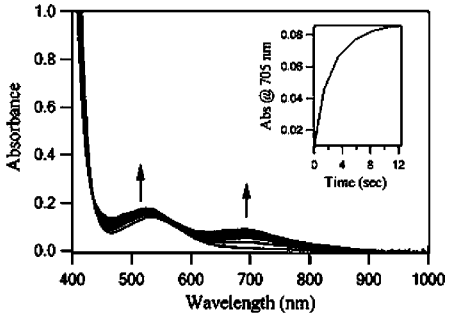

Figure 5. Time-resolved spectral changes in the reaction of **1** (2 mM) with 1 equiv of H_2O_2 in CH_3CN at 0 °C, monitored by stopped-flow spectrophotometry. Concentrations are listed before mixing. Inset: time course of the reaction monitored at 705 nm.

fairly broad, medium-intensity band was observed in the near-IR region (λ_{max} = 690 nm, $\varepsilon \approx 100$ M^{-1} cm^{-1}). This spectral feature is characteristic of low-spin nonheme iron(IV) oxo intermediates,[24,25] suggesting that an Fe^{IV}=O species has been formed in the reaction of **1** with H_2O_2. The accumulation of this species was a rapid process with a rate that depended linearly on the concentration of H_2O_2 (k_2 = 405 M^{-1} s^{-1}) (Supporting Information, Figure S4).

The lifetime of this intermediate at 0 °C was relatively short, and it further decreased from 2−3 min to several seconds as the concentration of H_2O_2 increased from its stoichiometric amount to a 10-fold excess with respect to iron complex. The growth and decay of the absorption band at 690 nm was accompanied by other spectral changes. Notably, another band, with $\lambda_{max} \approx 540$ nm, grew in the spectrum of the reaction mixture. Although the starting complex, **1**, also had an absorption band at 536 nm, albeit a weak one (ε = 148 M^{-1} cm^{-1}), the consumption of **1** did not result in the decay in absorbance intensity around 540 nm (Figure 5) because of the overlap with reaction intermediate(s) and product(s) absorbing in the same spectral range. Several iron complexes are known to have relatively intense optical bands in the 500−600 nm region, including Fe(III)-OOH intermediates[91−98] and iron(II) complexes with *Schiff* base macrocycles[65] that could result from ligand oxidation. Mass spectra of this resulting solution (m/z at 479.2, $[Fe^{II}(\mathbf{L1}-2H)(OTf)]^+$ and m/z at 477.2 $[Fe^{II}(\mathbf{L1}-4H)(OTf)]^+$) corresponded to the iron(II) complex with an oxidized ligand, suggesting that the ligand has been partially or fully oxidized upon mixing of **1** with different amount of H_2O_2. Ligand oxidation was not observed in the absence of H_2O_2.

Rapid formation of the presumed Fe^{IV}=O intermediate from **1** and H_2O_2 suggested that this species may be responsible for olefin epoxidation catalyzed by **1** and related Fe-PyMACs. However, an interplay of several reactions, including rapid ligand oxidation, in this seemingly simple system would complicate the study of Fe^{IV}=O and its role in catalytic substrate oxidations with hydrogen peroxide. Using oxidants other than H_2O_2 was expected to provide additional insight into ligand-based oxidation versus metal-based oxidation. Relatively mild oxidants, such as O_2 (air), were chosen to characterize spectroscopic changes due to ligand oxidation. On the other hand, strong oxygen atom donors, such as high-valent iodine-oxo species, provided alternative chemical methods of generating Fe^{IV}=O.

(b). Reaction with O_2. When complex **1** was exposed to air in acetonitrile solution, a slow reaction occurred. No near-IR bands appeared in this reaction, but the spectral changes in the 500−600 nm region were qualitatively similar to the ones observed in reaction of **1** with H_2O_2 (λ_{max} (ε, L mol^{-1} cm^{-1}): 355 (sh, 2440), 375 (2640), 492 (720), 529 (800)) after exposing **1** to air in CH_3CN overnight). The mass spectrum of this red solution (m/z at 479.2, $[Fe^{II}(L1-2H)(OTf)]^+$) corresponded to the iron(II) complex with a partially oxidized ligand. The formulation of this complex as **1c** is supported by its Mössbauer spectrum (Figure 6), with spectral parameters (δ

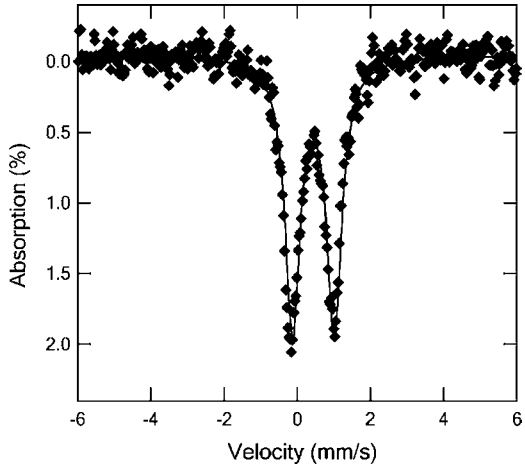

Figure 6. Zero-field Mössbauer spectrum of **1c** in frozen acetontrile solution acquired at 90 K. The solid line displays the least-squares fit to the spectrum, giving the parameters δ = 0.41(5) mm/s and ΔE_Q = 1.14(5) mm/s (Γ = 0.50 mm/s). The sample was obtained by oxidation of **1** in air overnight.

= 0.41(5) mm/s and ΔE_Q = 1.14(5) mm/s) consistent with a low-spin iron(II) configuration.[86−88] A small decrease in isomer shift with concomitant increase in quadrupole splitting, as compared with **1** (δ = 0.50(2) mm/s, ΔE_Q = 0.78(2) mm/s, see discussion above), is typical for iron macrocycles with an increasing degree of unsaturation, and the difference in ΔE_Q (0.3 mm/s) may correspond to one additional C=N bond as reported for a series of tetraazamacrocyclic iron(II) com-

dx.doi.org/10.1021/ic202435r | *Inorg. Chem.* 2012, 51, 5006−5021

plexes.[99] Stepwise oxidation of similar nickel(II) pyridine azamacrocycles with HNO_3 has been reported,[100] affording analogues of **1c** and **1e** (with nickel in place of iron). Analogous *Schiff* base complexes were observed during and after the reaction of **1** with hydrogen peroxide; mass spectrometry and UV−vis spectra indicated the formation of **1c** and **1e**.

Importantly, electrochemistry of the iron(II) complexes with partially and fully oxidized ligand, **1c** and **1e**, is qualitatively similar to that of **1**: both complexes exhibit reversible waves in their cyclic voltammograms at progressively positive potentials (Table 4, Supporting Information, Figure S5). It can be concluded that ligand oxidation does not destroy the macrocycle, and the resulting *Schiff* base macrocyclic complexes of iron retain the ability to undergo reversible oxidations/reductions.

Table 4. Redox Potentials of Iron(II) Complexes Studied in This Work

complex	$E_{1/2}$ adjusted vs Fc^+/Fc (V)	ΔE_p (V)	reversibility
1	0.49	0.055	R
1c	0.51	0.11	R
1e	0.62	0.034	R

(c). Reaction of 1 with Isopropyl 2-Iodoxybenzoate (iPr-IBX ester): Generation of Fe(IV) Intermediates. In search for clean methods of generating Fe^{IV}=O intermediates from **1**, an oxygen atom transfer to the Fe(II) center in **1** was attractive. Among oxygen atom transfer reagents, iodine-oxo compounds have been known to act as clean and efficient two-electron oxidants.[66,101,102] However, popular iodine(III)-oxo reagents, such as iodosobenzene (PhIO), suffer from low solubility in most organic solvents. Substituted iodosobenzenes with somewhat higher solubilities, such as 2,6-dimethyliodosylbenzene (Me2-PhIO),[103] are still less-than-optimal for the intended detailed kinetic studies of reactive intermediates, where broad concentration and temperature ranges had to be covered and low temperatures were often required. Unlike the majority of iodine(III) compounds, selected iodine(V) oxidants offered a combination of high reactivity with high solubility in common solvents (e.g., ca. 100 mM in CH_3CN at 25 °C).[102] In contrast to explosive Dess-Martin reagents (DMP) and related hypervalent compounds, recently reported esters of 2-iodylbenzoic acid (IBX esters) proved to be safe, thermally stable reagents that are easy to synthesize and handle.[66] Furthermore, IBX esters were successfully utilized in iron-catalyzed oxidations (e.g., iron-phthalocyanine catalyzed oxidation of alcohols[101] and anthracenes[104]). In the present work, we took advantage of the high solubility of isopropyl 2-iodoxybenzoate in acetonitrile (ca. 100 mM in CH_3CN at 25 °C)[66] and tested this reagent for the oxygen atom transfer to an iron(II) center in **1** at low-temperature. To the extent of our knowledge, this is the first report on applications of IBX esters for the generation of high-valent iron-oxo intermediates in nonheme iron systems.

Iron(II) complex **1** rapidly reacted with isopropyl 2-iodoxybenzoate; stopped-flow spectrophotometry was necessary to follow the initial steps of this process under most practically important reaction conditions. Changes in time-resolved UV−vis spectra with subsequent mass-spectrometric analysis allowed us to also identify iron-containing oxidation intermediates formed over longer time periods; a proposed reaction scheme for **1** upon addition of isopropyl 2-iodoxybenzoate is shown in Scheme 2. The rate of formation of **1b** was determined in stopped-flow experiments as described below.

Scheme 2. Proposed Reaction Steps for the Interaction of the Iron(II) Complex 1 with Isopropyl 2-Iodoxybenzoate[a]

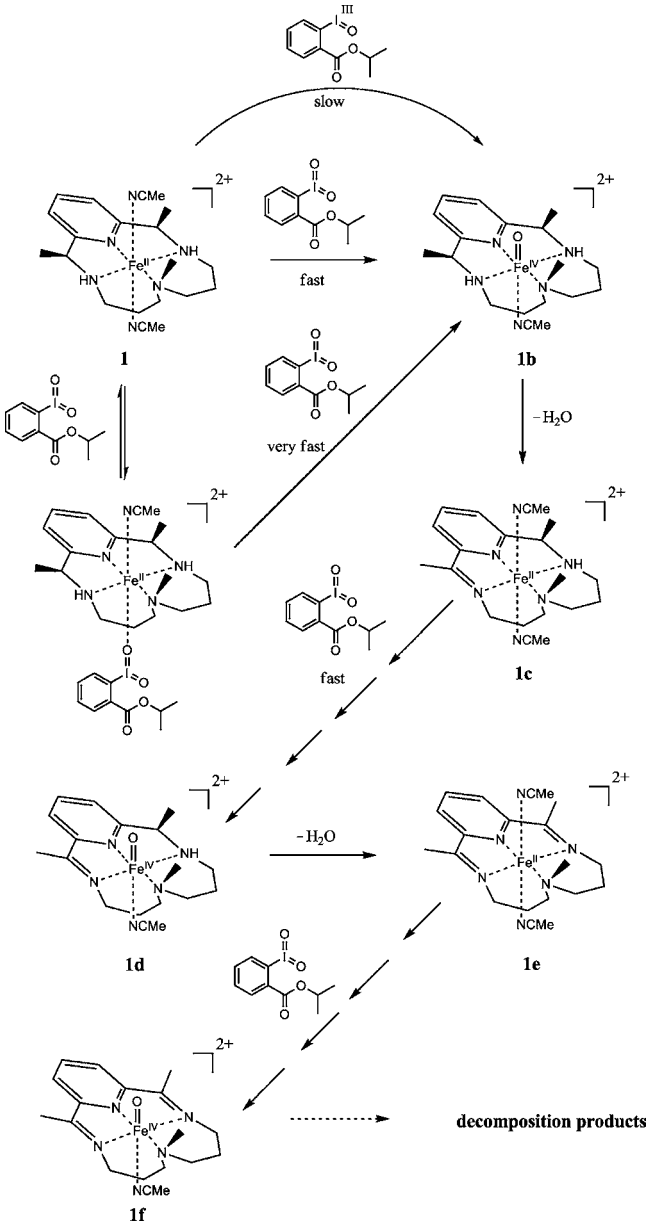

[a]The rate of formation of **1b** was determined by stopped-flow spectrophotometry.

Treatment of **1** (0.5 mM) with 1−18 equiv of isopropyl 2-iodoxybenzoate at low temperatures (from 0 to −40 °C) in CH_3CN resulted in the decay of the absorption band of **1** and a concomitant appearance of a new band with λ_{max} = 705 nm ($\varepsilon \approx 240\ M^{-1}\ cm^{-1}$) (Figure 7a). This chromophore indicated the formation of the corresponding ferryl complex, which showed the expected low-energy d−d transition band in the near-IR region, characteristic of an $S = 1$ oxoiron(IV) center.[105,106] ESI-MS of this green species exhibits peaks corresponding to $[Fe^{IV}(L1)(O)]^{2+}$, **1b** (Supporting Information, Figure S6). This intermediate was stable for several hours at −40 °C, but

dx.doi.org/10.1021/ic202435r | Inorg. Chem. 2012, 51, 5006−5021

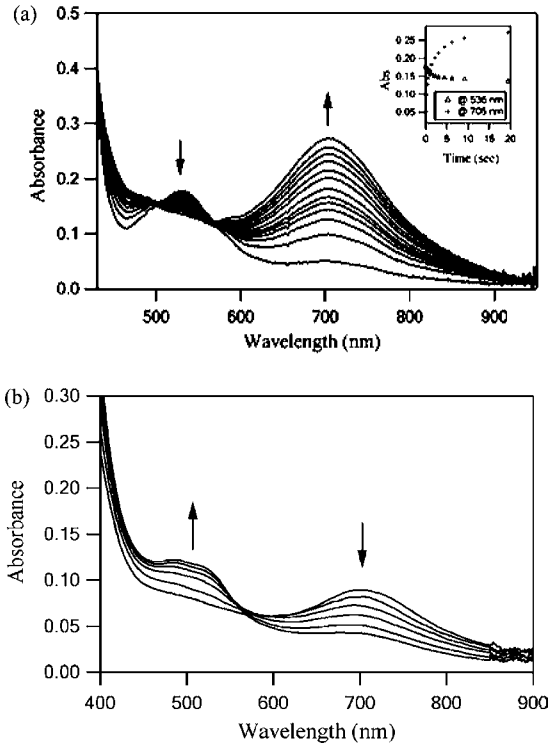

Figure 7. Reaction of **1** (2 mM) with 2 equiv of isopropyl 2-iodoxybenzoate in CH_3CN. (a) Stopped-flow spectral changes at −20 °C. Inset: time course of the reaction monitored at 536 and 705 nm. (b) UV−vis spectral changes at room temperature over 1 h.

decayed within 1 h at room temperature to a stable brick-red species (λ_{max} = 492 nm, with an additional shoulder at 523 nm, Figure 7b, consistent with the iron(II) complex with a partially oxidized ligand; mass spectrometry results support this formulation).

Mössbauer spectroscopy confirmed the formulation of **1b** as an $[Fe^{IV}(L1)(O)]^{2+}$ species. Figure 8 shows a zero-field Mössbauer spectrum of a frozen solution, ^{57}**1b**, generated from the reaction between ^{57}**1** (40% ^{57}Fe with respect to total iron content) and about 10-fold excess of isopropyl 2-iodoxybenzoate dissolved in CH_3CN at −40 °C. The raw data were fit to two quadrupole doublets (Figure 8). Approximately 31% of the spectral area consists of a quadrupole doublet (δ = 0.03(2) mm/s and ΔE_Q = 2.00(2) mm/s (Γ = 0.39 mm/s)) associated with the intermediate **1b**. The isomer shift of this doublet was in the range of the values reported for low-spin S = 1 iron(IV)-oxo complexes (δ = −0.04 to 0.19 mm/s).[21,24,25] Importantly, this isomer shift was significantly lower than the values typical of either Fe(II) or Fe(III) complexes. Relatively large quadrupole splitting is uncommon but not unprecedented for Fe(IV)=oxo complexes.[97,107−111] The remaining 69% of the spectral area exhibited Mössbauer parameters (δ = 0.40(2) mm/s and ΔE_Q = 0.50(2) mm/s) associated with the decomposition product. These spectral parameters corresponded best to low-spin iron(II) compounds, although they differed somewhat from the *Schiff* base products of ligand oxidation, **1c** or **1e**. One possible structure of this oxidation product(s) included coordination of the oxidant to the iron(II) center in **1c** or **1e** (although such complexes would be unstable, they may exist at low temperatures as transient species).

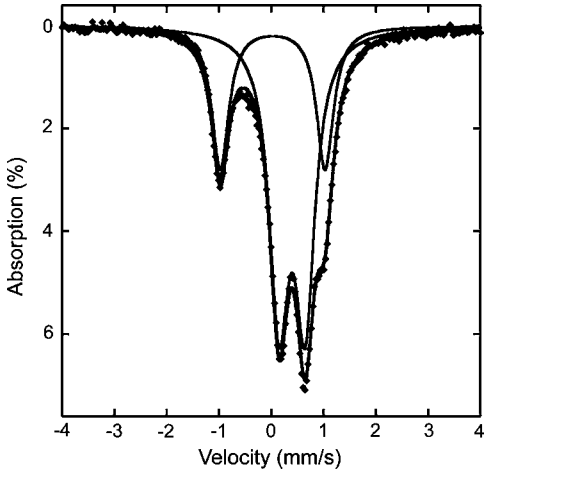

Figure 8. Zero-field Mössbauer spectrum of the intermediate ^{57}**1b** in a frozen acetonitrile solution acquired at 90 K. The solid line displays the least-squares fit to the spectrum. The fit for each subspectrum is also displayed (thin black lines).

Stopped-flow studies of the rapid reaction between **1** and *i*Pr-IBX ester (^{iPr}IOO) revealed a rather complicated, multistep process, which could be greatly simplified under certain reaction conditions (Figure 9). The simplest kinetics was

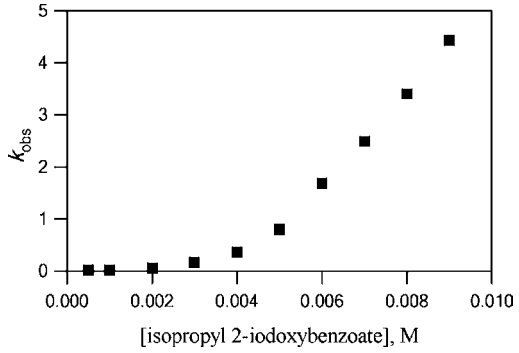

Figure 9. Plot of k_{obs} against the concentration of ^{iPr}IOO for the reaction of **1** (0.5 mM) with 1−18 equiv of ^{iPr}IOO in CH_3CN at −40 °C.

observed under large excess of ^{iPr}IOO at low temperature, where the decay of **1** (monitored at its λ_{max} = 536 nm) resulted in clean, mixed second-order (first order in each reactant) formation of **1b** (followed as a single-exponential growth of absorbance at 705 nm, $\varepsilon \approx 240$ M^{-1} cm^{-1}, Figure 7a). This allowed us to plot k_{obs} values for the reaction against varying excess ^{iPr}IOO concentrations (>8 equiv), outlined the rate law in eq 1, and allowed for determination of the second-order rate constant, k_2 = 1.65 × 10^3 M^{-1} s^{-1} at −40 °C.

$$-\frac{d[\mathbf{1}]}{dt} = \frac{d[\mathbf{1b}]}{dt} = k_{obs}[\mathbf{1}] = k_2[\mathbf{1}][\text{isopropyl 2-iodoxybenzoate}]_{(\text{beyond 8 equiv})} \quad (1)$$

Acquisition of kinetic data for the reaction of **1** (0.5 mM) with an 8-fold excess of ^{iPr}IOO over a range of temperatures (−40 to −25 °C) afforded a linear Arrhenius plot (Supporting

dx.doi.org/10.1021/ic202435r | Inorg. Chem. 2012, 51, 5006−5021

Information, Figure S10b) and yielded the effective activation energy of $E_a^{\ddagger}$ = 35 kJ/mol.

At longer reaction times, and especially at higher temperature, the second, slower process becomes apparent, and mass spectrometry clearly indicated partial ligand oxidation (Supporting Information, Figure S7). Subsequent reaction of **1c** with excess $^{i\mathrm{Pr}}$IOO resulted in the accumulation of the modified high-valent iron-oxo intermediate, **1d** (λ_{max} = 696 nm), which, in turn, could further react with excess oxidant, yielding **1e** and **1f** (Scheme 2, Supporting Information, Figures S8, S9). Importantly, partial ligand oxidation did not lead to complete decomposition of the macrocycle; instead, the iron(II) *Schiff* base macrocycles form, and continued to serve as precursors for the (L)Fe^{IV}=O species. The complexes with oxidized ligands also retained reversible or quasi-reversible one-electron redox couples (LFe^{III}/LFe^{II}) displayed by **1**, at somewhat more positive potentials because of relative stabilization of Fe(II) by the unsaturated macrocycles (Supporting Information, Figure S5).

Ligand oxidation could be partially suppressed by using smaller amounts of the oxygen atom donor, $^{i\mathrm{Pr}}$IOO. However, oxygen atom transfer with 0.5−6 equiv of $^{i\mathrm{Pr}}$IOO with respect to **1** was significantly slower than the reactions with a larger excess of $^{i\mathrm{Pr}}$IOO (Figure 7a, Figure 9, Supporting Information, Figure S10). This deviation from linearity in the plots of k_{obs} vs the concentration of $^{i\mathrm{Pr}}$IOO suggested that the initial coordination of the oxidant to the iron center may facilitate oxygen atom transfer from another molecule of $^{i\mathrm{Pr}}$IOO. Additionally, the second oxygen atom of the oxidant is transferred to the iron center in a slower process. Despite these complications, stoichiometric or substoichiometric amounts of $^{i\mathrm{Pr}}$IOO cleanly and quantitatively transferred an oxygen atom to **1** within minutes at −40 °C (Supporting Information, Figures S10, S11) and even faster at higher temperatures. Spectrophotometric titrations showed that both oxygen atoms of $^{i\mathrm{Pr}}$IOO were eventually transferred to the iron center. Therefore, 0.5 mol of isopropyl 2-iodoxybenzoate were needed for essentially quantitative formation of **1b**. Although complete kinetic and mechanistic analyses of the reaction between **1** and $^{i\mathrm{Pr}}$IOO were precluded by the multiple consecutive and parallel processes involved in this transformation (Scheme 2), the limiting cases proved to be revealing. With a large excess of $^{i\mathrm{Pr}}$IOO, one oxygen atom of the oxidant was rapidly transferred to the iron center, cleanly generating (L)Fe^{IV}=O (**1b**); initial coordination of another molecule of $^{i\mathrm{Pr}}$IOO likely accelerated this process. However, in situations where excess oxidant had to be avoided (e.g., in detailed studies of substrate oxidations with iron(IV) intermediates), high-valent iron(IV)-oxo species could be produced, in a somewhat slower multistep process, by sequentially transferring both oxygen atoms from 0.5 mols of $^{i\mathrm{Pr}}$IOO per mole of the iron(II) complex **1**. Partially oxidized macrocycles were capable of supporting iron(IV)-oxo intermediates, such as **1d** and **1e** (Supporting Information, Figure S12).

Reactivity of Oxoiron(IV) in Triarylphosphine Oxidation. Identification of the iron(IV)-oxo intermediates in reactions of **1** with oxygen atom donors (such as IBX ester) and optimizing the reaction conditions that produce Fe^{IV}=O in high yields set the stage for understanding the reactivity of these intermediates in oxygen atom transfer to substrates. Phosphines are frequently used as oxygen atom acceptors in reactions with metal-oxo complexes. Although phosphine oxidation does not represent a synthetic challenge, these substrates are nevertheless useful as mechanistic probes in studying electronic and steric effects in oxygen atom transfer reactions.

Triarylphosphines were found to cleanly react with **1b** generated from complex **1** and $^{i\mathrm{Pr}}$IOO (premixed in a 2:1 molar ratio). To avoid direct interaction between PAr_3 and $^{i\mathrm{Pr}}$IOO, stoichiometric or substoichiometric amounts of the oxidant were used, and sufficient incubation times, determined from independent single-mixing stopped-flow experiments, ensured quantitative incorporation of both oxygen atoms of $^{i\mathrm{Pr}}$IOO into the Fe^{IV}=O intermediate **1b**. Upon addition of PPh_3 to the preformed solution of **1b** in the stopped-flow instrument, a relatively fast and smooth single-exponential decay of the absorption band at λ_{max} = 705 nm occurred (Figure 10-a),

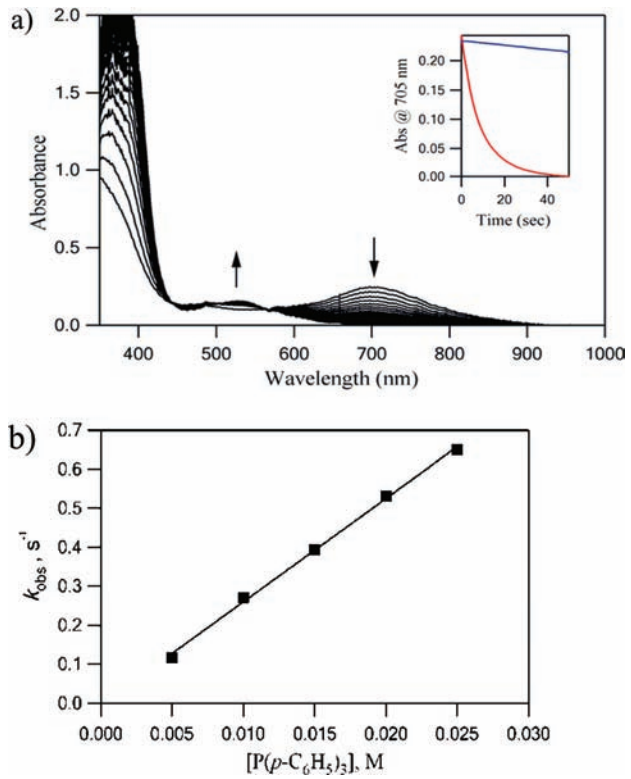

Figure 10. Reaction of **1b** with triphenylphosphine. (a) Time-resolved spectra upon addition, in the second mixing, of 5 equiv of PPh_3 (40 mM) to **1b** pregenerated by reaction of **1** (4 mM) with $^{i\mathrm{Pr}}$IOO (2 mM) in CH_3CN with 6 s age time; CH_3CN, 0 °C, reaction time 50 s. Inset: time course of the reaction monitored at 705 nm (red line) and self-decay of **1b** in the absence of PPh_3 (blue line). (b) Determination of the second-order rate constant by plotting k_{obs} against concentration of $P(C_6H_5)_3$ (5−25 equiv) at 0 °C; phosphine concentrations in the cell during the reaction are shown on the *x*-axis of the plot.

quantitatively yielding Ph_3PO (as analyzed by GC-MS). The observed pseudo-first order rate constant increased linearly with increasing concentrations of PPh_3 (Figure 10b), indicating first order in this reagent and second order overall:

$$\text{Rate} = k_2[\mathbf{1b}][PPh_3]$$

The second order rate constant at 0 °C was found to be k_2 = 26.5 M^{-1} s^{-1} (Table 5), and it decreased at lower temperatures (down to −20 °C) (Supporting Information, Figure S14b), yielding the activation parameters summarized in Table 5. A

dx.doi.org/10.1021/ic202435r | *Inorg. Chem.* 2012, 51, 5006−5021

Table 5. Kinetic Parameters for Substrate Oxidation with 1b

	k_2 (M^{-1} s^{-1}) 273 K	$\Delta H^{\ddagger}$ (kJ/mol)	$\Delta S^{\ddagger}$ (J/mol K)	$\Delta G^{\ddagger}$ (kJ/mol) 298 K
PPh_3 oxidation	26.5	53	−25	60
cyclooctene epoxidation	0.45 (0.17[a])	23.0	−169	73

[a]This value was acquired from the reaction of substrate with **1b** generated by premixing of complex **1** with H_2O_2.

negative value of activation entropy suggests an associative rate-limiting step in phosphine oxidation.[111]

In the presence of excess phosphine, ferryl(IV) species were reduced to the starting iron(II) complex **1**, as followed from the final UV−vis (Figure 10a) and mass spectra (m/z = 481.2). When 1 equiv of PPh_3 was used, the reaction was relatively slow and competing ligand oxidation became apparent (Supporting Information, Figure S14), as evidenced by the growth of the absorption bands at 492 and 523 nm and the appearance of the peak at m/z = 479.2 (**1c**) in the mass spectrum.

The fast reduction of **1b** into **1** upon addition of excess PPh_3 allowed us to perform repeated oxidation−reduction cycles (monitored by UV−vis) (Supporting Information, Figure S15). To a solution containing **1** and 50 equiv of PPh_3 in CH_3CN, 1 equiv of ^{iPr}IOO was added, resulting in a rapid formation the green species which immediately decayed, forming a red solution with a UV−vis spectrum nearly identical to that of **1**. This sequence of reactions was repeated five times; stepwise addition of the oxidant was necessary to prevent direct oxidation of PPh_3 with ^{iPr}IOO. In each addition, another equivalent of ^{iPr}IOO again gave a flash of green intermediate that decayed into red product. The UV−vis monitoring showed that the spectra of the resulting red solutions remained essentially unchanged after repeated cycles. This suggested that the iron(IV)-oxo could be converted back to the original iron complex with multiple turnovers when the reduction step was fast.

Iron(IV)-oxo species behaved as electrophilic oxidants in several reported examples of substrate oxidations.[34,112−114] To determine whether the new iron-oxo intermediate **1b** followed this trend, substituted triarylphosphines were used as substrates. In the electrophilic oxidation of triarylphosphines, the rates were expected to increase with the electron-donating properties of the *para* substituent.[115−117] The kinetics of the reactions of a series of derivatives of PPh_3 with electron-withdrawing (F, Cl) and -donating (OMe, Me) *para* phenyl substituents were examined.

The reactivity of several investigated *para*-substituted phosphines increased with the electron-donating properties of the substituents. For this admittedly limited set of substrates, this trend is graphically reflected in the correlation between the reaction rates and the values of Hammett parameters, σ (ρ = −1.05, R^2 = 0.789; the presence of three substituted aryl groups in the molecules of substrates accounts for a factor of 3 in plotting k_{obs} against 3 σ; Figure 11). The observed trend implies the electrophilic character of the oxo group of the nonheme oxoiron(IV) complex **1b** and positive charge buildup on phosphorus in the PPh_3 oxygenation reactions. Thus, the nonheme oxoiron(IV) complex **1b** are capable of oxygenating substrates via an electrophilic oxidation mechanism.[118] Analogous electrophilic character of iron(IV)-oxo species was observed in sulfoxidation[34,112] and aromatic hydroxylation reactions.[113,114]

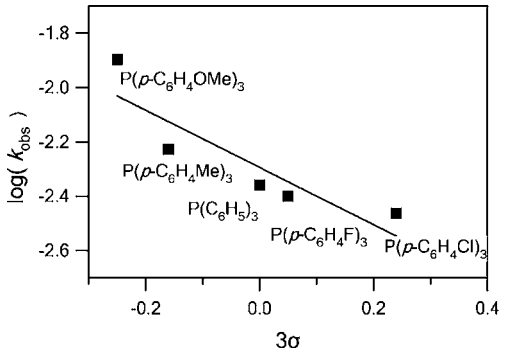

Figure 11. Hammett correlation for the observed rate constant of triarylphosphine oxidations with **1b** (generated by the reaction of **1** (4 mM) with ^{iPr}IOO (2 mM) in CH_3CN with 6 s age time); 1 equiv of PAr_3 (4 mM) was added, in the second mixing, at 0 °C. ρ = −1.05 (R^2 = 0.789).

Reactivity of Oxoiron(IV) in Olefin Epoxidation. To understand the potential role of iron(IV) intermediates in olefin epoxidations with hydrogen peroxide catalyzed by complex **1**, the reactivity of independently generated iron-(IV)-oxo species with olefins was studied experimentally. Similarly to phosphine oxidation experiments described above, ferryl(IV) species were obtained in the reaction of **1** with ^{iPr}IOO. Identifying kinetically competent intermediates in catalytic epoxidations required measurements of individual reaction rates under various conditions. Ferryl(IV) intermediates were subjected to reactions with cyclooctene, and reaction rates were determined by the addition of substrate (cyclooctene) to the preformed iron(IV)-oxo species in detailed double-mixing stopped-flow experiments. In the first mixing step, CH_3CN solutions of **1** (4 mM) and 0.5 equiv of isopropyl 2-iodoxybenzoate were combined at 0 °C and incubated for 6 s to ensure maximum formation of iron(IV)-oxo while avoiding excess oxidant. An acetonitrile solution of substrate (cyclooctene, 40 mM) was then mixed in, causing the decay of the absorption band of the iron(IV) intermediate **1b** (λ_{max} = 705 nm), with a clear isosbestic point at 555 nm (Figure 12a). Under the same conditions, **1b** remained stable upon mixing with CH_3CN in a control reaction. These results demonstrated that the intermediate oxoiron(IV) reacted with cyclooctene. The kinetics of cyclooctene oxidation was monitored by the disappearance of **1b**. The rate of this process does not depend on the concentrations of reagents that were used to generate **1b**; experiments at substoichiometric ^{iPr}IOO (less than 0.3 equiv with respect to **1**) and longer incubation times ensure the dominance of **1b** as the oxidant. The rate of epoxidation was investigated over a range of substrate concentrations (excess cyclooctene was always used); pseudo-first order fitting of the kinetic data allowed us to determine k_{obs} values, which increased linearly with cyclooctene concentration (20−100 equiv) (Figure 12b), indicating the second-order rate law (first-order in each reactant, eqs 2, 3).

$$-\frac{d[\mathbf{1b}]}{dt} = \frac{d[\mathbf{1c}]}{dt} = k_{obs}[\mathbf{1b}] = k_2[\mathbf{1b}][\text{cyclooctene}] \quad (2)$$

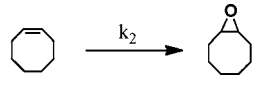

(3)

Electrophilic oxidant (L1)Fe^{IV}=O transfers its oxygen atom to the C=C double bond of the olefin substrate, most likely via a

dx.doi.org/10.1021/ic202435r | Inorg. Chem. 2012, 51, 5006−5021

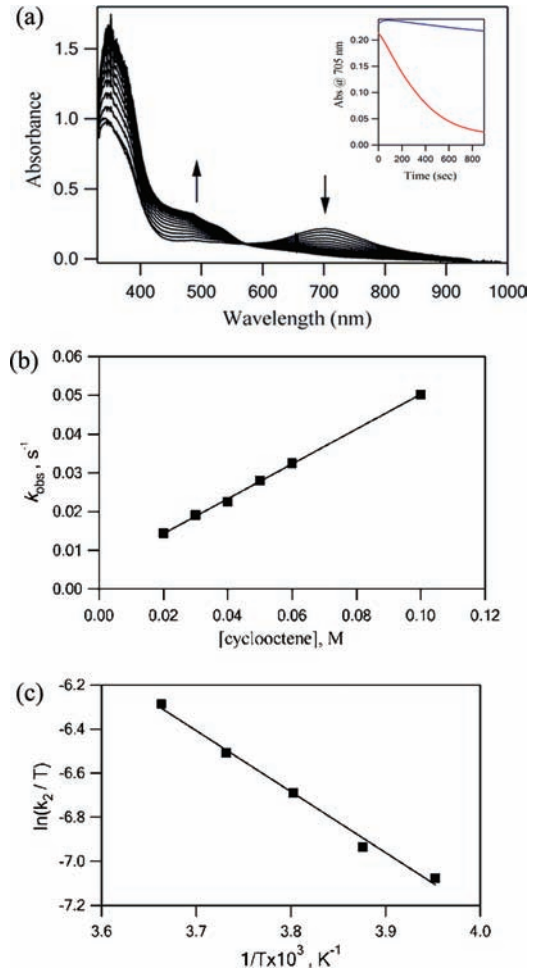

Figure 12. (a) Time-resolved spectral changes upon mixing of **1b** (generated by reaction of **1** (4 mM) with ^{iPr}IOO (2 mM) in CH_3CN with 6 s age time) with 20 equiv of cyclooctene (40 mM) in CH_3CN over 900 s at 0 °C. Inset: time course of the reaction monitored at 705 nm (red line) and a control experiment (self-decay of **1b** solution, blue line). (b) Determination of the second-order rate constant by plotting k_{obs} against cyclooctene concentration (20−100 equiv); 0 °C. (c) Eyring plot for the reaction of **1b** with 60 equiv of cyclooctene (−20 to 0 °C) in CH_3CN.

concerted pathway, as follows from the retention of stereochemistry in epoxidation of *cis*-2-heptene into *cis*-epoxide (Table 3). The second-order rate constant for cyclooctene oxidation, k_2 = 0.45 M^{-1} s^{-1} at 0 °C, was significantly lower than the rate constant for the oxidation of PPh_3 discussed above (Table 5). The temperature dependence (T = −20 to 0 °C) of the second-order rate constant fits the linear form of the Eyring equation, giving the activation parameters of $\Delta H^{\ddagger}$ = 23 kJ/mol and $\Delta S^{\ddagger}$ = −169 J/(mol K), typical of associative processes (Figure 12c).[106,114] A similar approach has been applied to the reaction of **1** and H_2O_2, showing k_2 = 405 M^{-1} s^{-1} at 0 °C in single mixing of **1** and H_2O_2 (1−20 equiv) (Supporting Information, Figure S13a) and k_2 = 0.17 M^{-1} s^{-1} at 0 °C in cyclooctene oxidation (Supporting Information, Figure S13b, Table 4), which is comparable to the reaction of **1** and ^{iPr}IOO.

Kinetic experiments unambiguously proved bimolecular decay of the iron(IV)-oxo intermediate upon reaction with cyclooctene. In separate benchtop experiments, Fe(IV)═O species were generated from **1** and ^{iPr}IOO, treated with cyclooctene, and the products of these reactions were analyzed

Table 6. Olefin Epoxidation Reaction with Isopropyl 2-Iodoxybenzoate[a]

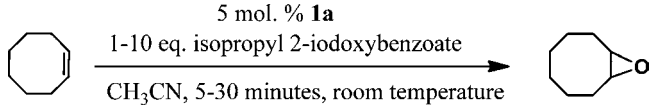

oxygen-donor (isopropyl 2-iodoxybenzoate)[b]	reaction time (min)	moles of epoxide[a]
1 equiv	5	0.2
1 equiv	30	0.81
2 equiv	5	0.45
2 equiv	30	1.58
5 equiv	5	0.67
5 equiv	30	3.3
10 equiv	5	0.73
10 equiv	30	3

[a]Moles of epoxide per mole of catalyst. [b]Catalyst:cyclooctene:isopropyl 2-iodoxybenzoate =1:20:(1/2/5 or 10).

and quantified by GC-MS (Table 6). Control experiments showed that ^{iPr}IOO did not oxidize cyclooctene under the reaction conditions in the absence of **1**.

Equimolar amount of ^{iPr}IOO with respect to **1** afforded 0.2 mol of cyclooctene epoxide in 5 min (0 °C, 20-fold excess of olefin). However, epoxide yield increased over time, reaching 0.8 mol per mol of **1** after 30 min. Epoxidation appeared to be slow under experimental conditions, but the epoxidation time scale was consistent with the rate of cyclooctene-induced decay of the iron(IV)-oxo intermediate determined from stopped-flow experiments. No diol was produced, providing indirect evidence for water-assisted pathways for diol formation in catalytic olefin oxidations with H_2O_2.[119] Using 2 equiv of ^{iPr}IOO, the reaction afforded up to 1.6 mols of epoxide in 30 min, and even larger excess of oxidant (5 or 10 equiv) increased the epoxide yield to about 3 mols per mole of **1**. These results clearly showed the decay reaction upon addition of cyclooctene to the preformed **1b** yielded the corresponding epoxide in about 30 min; less than quantitative yields of epoxide with respect to oxidant (Table 6) could be attributed to partial ligand oxidation (**1c** and **1e** were detected by mass-spectrometry).

To assess the effects of ligand oxidation on the reactivity of iron(IV)-oxo species with olefins, cyclooctene epoxidation with ^{iPr}IOO was performed in the presence of **1c** or **1e**. The complex with a single C═N bond, **1c**, yields 0.7 mols of epoxide using excess oxidant. Moreover, this ligand oxidation reaction upon the addition of cyclooctene to preformed **1d** (generated by premixing **1c** and 1 equiv of ^{iPr}IOO) was also observed in stopped-flow experiments (Supporting Information, Figure S16). These results demonstrated that **1d** could transfer an oxygen atom to cyclooctene to produce epoxide, although additional ligand oxidation (leading to **1e**) competed with oxygen atom transfer to the substrate. Therefore, three types of macrocyclic oxoiron(IV) species: **1b**, **1d**, and **1f** consecutively formed, and each could function as an effective oxygen-atom transfer reagent that can attack cyclooctene to form epoxide. The ability of **1d** or **1f** to oxidize substrates does not compromise the kinetic results described above for the reactions of **1b** with cyclooctene because the ferryl species

dx.doi.org/10.1021/ic202435r | *Inorg. Chem.* 2012, 51, 5006−5021

supported by partially oxidized macrocycles do not form with substoichiometric amounts of oxidant, especially on the time scale of the stopped-flow measurements. The reactivity of ferryl(IV) intermediates with respect to cyclooctene appeared to decrease as the number of C=N bonds in the macrocycle increased and the number of available secondary amino groups decreased. Nevertheless, ligand oxidation of FePyMACs, such as **1**, did not lead to complete destruction of the catalyst. Instead, partially oxidized *Schiff* base pyridine-containing macrocycles were capable of supporting high-valent iron-oxo intermediates that carry out relatively slow (minutes at room temperature) but high-yielding (nearly quantitative in case of **1b**) transfer of an oxygen atom from the oxidant to the olefin substrate.

DISCUSSION

Iron complexes with aminopyridine macrocycles are known to be catalytically active in a number of "green" catalytic oxidations.[49,54−57] For example, complexes **2** and **3** (Figure 2) were found to be efficient catalysts of olefin epoxidation with hydrogen peroxide, a nontoxic oxidant that produces water as the only byproduct.[65] A related macrocyclic complex with a 12-membered ligand containing two pyridine rings (Figure 1) catalyzes efficient and selective olefin dihydroxylation with oxone in water.[120] An iron(III) complex with a nonmethylated analogue of **L1**, $[Fe(CRH)]Cl_2(BF_4)$, is known to be one of the best models of catalase,[121−125] and hydrogen peroxide decomposition is thought to involve an Fe(IV) intermediate.[126] In the present work, an iron(II) complex with a tetradentate aminopyridine macrocycle **L1**(complex **1**) was found to display modest catalytic activity in olefin epoxidation with hydrogen peroxide. Complex **1** provided a convenient platform for exploring the role of high-valent iron-oxo intermediates in stoichiometric and catalytic substrate oxidations.

Complex **1** contained low-spin iron(II) in a pseudo-octahedral geometry, as determined by X-ray crystallography. Magnetic susceptibility measurements and Mössbauer spectroscopy confirmed that low-spin configuration of Fe(II) was retained in acetonitrile solutions. Electrochemistry revealed reversible one-electron oxidation/reduction of the iron center in **1**, with $E_{1/2}$ = 0.49 V vs Fc^+/Fc, a value very similar to the half-wave potentials of related macrocyclic complexes such as **2** and a protonated form of **3**.[65] Reversibility of repeated electrochemical one-electron oxidations demonstrated the stability of the ligand **L1** on the cyclic voltammetry time scale. However, chemical oxidations with a mild oxidant, air oxygen, led to a slow (several hours) partial ligand oxidation, affording iron(II) complexes with *Schiff* base analogues of **L1** (complexes **1c** and **1e**, Figure 7, Scheme 2). Fortunately, the macrocycle remained intact, and amenable to reversible redox processes at the metal center.

Reaction of the iron(II) complex **1** with hydrogen peroxide, monitored by the stopped-flow method, afforded a mixture of several colored intermediates, including a species with an optical spectrum typical of low-spin iron(IV) complexes (λ_{max} = 705 nm, ε = 240 M^{-1} cm^{-1}, Figure 5). Formation of iron(IV) intermediates in reactions of iron(II) or iron(III) complexes with hydroperoxides is well-documented.[56,91,96,97,127,128] Generally accepted mechanisms for the Fe(IV) formation assume the intermediacy of the Fe(III)-(hydro)peroxo intermediates:[129,130]

$$(L)Fe^{II} + \frac{1}{2}ROOH \rightarrow (L)Fe^{III}(OOR)$$

$$(L)Fe^{III}(OOR) \rightarrow (L)Fe^{IV}{=}O + ROO\cdot$$

In our experiments, an iron(III)-hydroperoxo intermediate was not directly observed, suggesting that this species, if formed, rapidly undergoes O−O bond cleavage prior to the rate-determining step. Detailed kinetic experiments revealed the role of iron(IV) species in catalytic olefin epoxidations by determining the rates of individual reaction steps; a similar approach was used by the van Eldik group in the studies of catalytic oxidations with metalloporphyrins .[131,132]

Accumulation of the presumed Fe(IV)-oxo intermediate in the reaction of **1** with H_2O_2 was rapid (k_2 = 405 M^{-1} s^{-1} at 0 °C); the time scale of this process (Figure 5) was well within 5 min, the typical time used in olefin epoxidation experiments, suggesting that the Fe(IV)-oxo intermediate, **1b**, may be involved in catalytic epoxidations with H_2O_2. Unfortunately, ligand oxidation occurs concurrently with the buildup of the Fe(IV)-oxo intermediate upon interaction of **1** with hydrogen peroxide, thus complicating direct studies of the reactivity of Fe(IV) generated in this system.

Oxygen atom transfer reagents are often used to cleanly produce high-valent metal-oxo species. In our experiments, a rapid and clean reaction of **1** with a potent oxidant, isopropyl 2-iodoxybenzoate,[66] afforded an iron(IV) species that was characterized by UV−vis, Mössbauer, and mass spectrometry. The transfer of the first oxygen atom from the iodine(V) reagent, ^{iPr}IOO, occurred rapidly at or below room temperature (k_2 = 1654 M^{-1} s^{-1} at −40 °C):

$$(L)Fe^{II} + {}^{iPr}I^{V}OO \rightarrow (L)Fe^{IV}{=}O + {}^{iPr}I^{III}O$$

It appears that the coordination of ^{iPr}IOO to the iron(II) center in **1** accelerated the oxygen atom transfer process. It is also likely that ^{iPr}IOO and/or ^{iPr}IO coordinated to the Fe(IV)-oxo intermediate, similar to coordination of anions to high-valent iron(IV) complexes supported by other polyamine- or aminopyridine ligands.[17,24,27,37,58,133] Under stoichiometric or substiochiometric conditions, the reaction between **1** and ^{iPr}IOO was relatively slow (but still fast enough to reach the maximum accumulation of Fe^{IV} in 20 s at −20 °C, Figures 7a), and both oxygen atoms were being transferred from the oxidant to the iron(II) center. Having access to the Fe(IV)-oxo intermediate allowed us to investigate its reactivity. Quantitative data on the reactivity of ferryl(IV) intermediates in nonheme iron chemistry are still limited.[29,31,58,111,134]

Similarly to other ferryl(IV) species,[24,27,31,42,58] **1b** cleanly reacted with triarylphosphines, forming the corresponding phosphine oxides. Varying the electronic properties of substituents on the aryl rings revealed the electrophilic nature of the oxidant **1b**, as followed from the Hammett correlation with negative ρ (Figure 12). Analogous Hammett correlations were previously found for oxidations of sulfides,[34,112] phosphines,[115−117] and other organic substrates,[113,114] confirming the electrophilic nature of nonheme ferryl intermediates. The rate constant for the reaction of **1b** with triphenylphosphine, 26.5 M^{-1} s^{-1} at 0 °C, was comparable to the analogous values of the rate constants obtained with related nonheme iron complexes. For example, the first crystallographically characterized nonheme iron(IV) complex with tetramethylcyclam (TMC, Figure 1) reacted with PPh_3 about five times slower than **1b** (k_2 = 5.7 M^{-1} s^{-1} at 0 °C, for TMC[134]). Fairly rapid

dx.doi.org/10.1021/ic202435r | Inorg. Chem. 2012, 51, 5006−5021

oxidation of PPh_3 with **1b** and full regeneration of **1** in this process led to the possibility of performing multiple turnovers in PPh_3 oxidations with ^{iPr}IOO in the presence of substoichiometric amounts of **1**.

Rather high activity of ferryl species supported by aminopyridine macrocycle **L1** suggested that this intermediate might play an important role in catalytic olefin epoxidations. In a series of kinetic experiments, we found that **1b** reacted with cyclooctene (k_2 = 0.45 M^{-1} s^{-1} at 0 °C), forming epoxide. The time scale of cyclooctene oxidation with the Fe(IV)-oxo intermediate under catalytically relevant concentration conditions, about 100 s at room temperature, was comparable to the typical time of catalytic epoxidations with H_2O_2 (5 min). Interestingly, the rate constant of olefin epoxidation with **1b** generated from **1** and ^{iPr}IOO was very close to the value of the rate constant in the system where **1b** was generated from **1** and H_2O_2 (Table 4). This suggested that cyclooctene epoxidation was likely performed by ferryl(IV) species itself, rather than by other oxidant-derived intermediates (e.g., macrocycle adducts with the oxidant, or hydroxyl radicals). Independently determined rates of ferryl(IV) formation and its subsequent reaction with cyclooctene confirmed that the Fe(IV)-oxo species **1b** was a kinetically competent intermediate for cyclooctene epoxidation at room temperature; a similar approach, measuring the rates of individual reaction steps to identify a kinetically competent catalytic intermediate, was used by van Eldik and co-workers in their analysis of heme-catalyzed substrate oxidations.[131,132]

A catalytic cycle for substrate oxidation with H_2O_2 in the presence of **1** is depicted in Scheme 3. It should be noted that

Scheme 3. Catalytic Cycle for Substrate Oxidation with H_2O_2/^{iPr}IOO in the Presence of 1

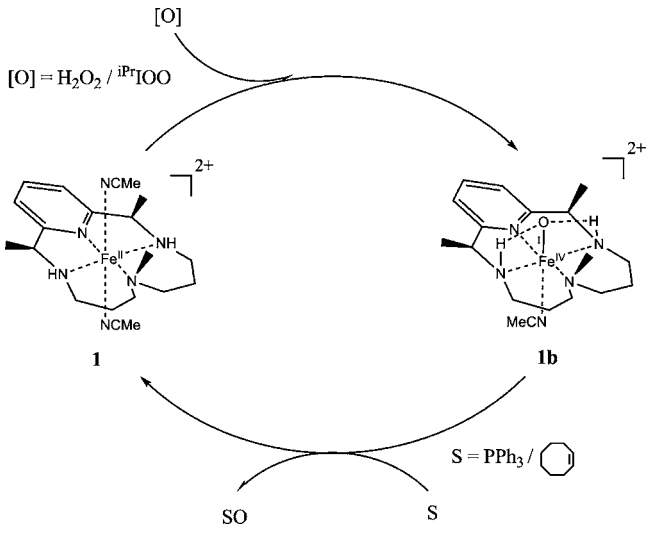

triphenylphosphine and cyclooctene, two substrates that can certainly be oxidized by Fe(IV)-oxo intermediate **1b**, are strong oxygen atom acceptors. Still, the ability of **1b** to epoxidize cyclooctene is notable, as several other nonheme ferryl(IV) species do not transfer an oxygen atom to olefins.[56] The iron(IV)-oxo moiety in **1b** may be activated by intramolecular hydrogen bonding to the NH-groups of the macrocycle (Scheme 3). Close proximity of the NH−hydrogens from the macrocycle also facilitate a competing reaction- hydrogen atom abstraction- yielding *Schiff* base complexes **1c** and **1e**. With good reducing agents as substrates, ligand oxidation does not occur (as was seen for triarylphosphine oxidations) or occurs slowly, affording both the substrate oxidation products and the oxidized (yet still somewhat reactive) *Schiff* base macrocycles (as was observed for cyclooctene). Fully oxidized macrocycle **1e**, lacking NH−groups, is much less reactive in olefin epoxidation than the parent complex **1**. These observations parallel previously reported data on olefin epoxidations; for example, iron cyclam was catalytically active in olefin epoxidations with H_2O_2, but the analogous complex with tetramethylcyclam (TMC) was inactive.[135] For the PyMAC complexes described in this work, the ferryl(IV) intermediate is competent in oxidations of selected substrates (triarylphosphines and cyclooctene). However, ferryl(IV) does not have to be the sole intermediate involved in substrate oxidations with H_2O_2 catalyzed by iron PyMACs; investigation into the mechanisms of more challenging oxidations are currently in progress.

■ ASSOCIATED CONTENT

Supporting Information

Crystallographic data in CIF format. Further details are given in Table S1 and Figures S1−S16. This material is available free of charge via the Internet at http://pubs.acs.org.

■ AUTHOR INFORMATION

Corresponding Author

*E-mail: elena.rybak-akimova@tufts.edu.

Notes

The authors declare no competing financial interest.

■ ACKNOWLEDGMENTS

This work was supported by the U.S. Department of Energy, Office of Basic Energy Science, Grant DE-FG02-06ER15799. The NMR facility, the ESI-MS spectrometer, and rapid kinetic instrumentation at Tufts were supported by the NSF (Grants CHE-9723772, MRI CHE 0821508, MRI CHE 0320783, and CHE 0639138). We thank Prof. Stephen Lippard (MIT) for generously allowing us to use Mössbauer spectrometer in his laboratories.

■ REFERENCES

(1) Lippard, S. J.; Berg, J. M. In *Principles of Bioinorganic Chemistry*; University Science Books: Mill Valley, CA., 1994.
(2) Sono, M.; Roach, M. P.; Coulter, E. D.; Dawson, J. H. *Chem. Rev.* **1996**, *96* (7), 2841−2887.
(3) Que, L., Jr. *J. Biol. Inorg. Chem.* **2004**, *9* (6), 643.
(4) Que, L., Jr.; Ho, R. Y. N. *Chem. Rev.* **1996**, *96* (7), 2607−2624.
(5) Solomon, E. I.; Brunold, T. C.; Davis, M. I.; Kemsley, J. N.; Lee, S. K.; Lehnert, N.; Neese, F.; Skulan, A. J.; Yang, Y. S.; Zhou, J. *Chem. Rev.* **2000**, *100* (1), 235−349.
(6) Lange, S. J.; Que, L., Jr. *Curr. Opin. Chem. Biol.* **1998**, *2* (2), 159−172.
(7) Bugg, T. D. *Curr. Opin. Chem. Biol.* **2001**, *5* (5), 550−555.
(8) Westerheide, L.; Pascaly, M.; Krebs, B. *Curr. Opin. Chem. Biol.* **2000**, *4* (2), 235−241.
(9) Wallar, B. J.; Lipscomb, J. D. *Chem. Rev.* **1996**, *96* (7), 2625−2658.
(10) Costas, M.; Mehn, M. P.; Jensen, M. P.; Que, L., Jr. *Chem. Rev.* **2004**, *104* (2), 939−986.
(11) Tshuva, E. Y.; Lippard, S. J. *Chem. Rev.* **2004**, *104* (2), 987−1011.
(12) Hong, S.; Lee, Y. M.; Shin, W.; Fukuzumi, S.; Nam, W. *J. Am. Chem. Soc.* **2009**, *131* (39), 13910−13911.

(13) Yoon, J.; Wilson, S. A.; Jang, Y. K.; Seo, M. S.; Nehru, K.; Hedman, B.; Hodgson, K. O.; Bill, E.; Solomon, E. I.; Nam, W. *Angew. Chem., Int. Ed.* **2009**, *48* (7), 1257−1260.
(14) Lee, Y. M.; Hong, S.; Morimoto, Y.; Shin, W.; Fukuzumi, S.; Nam, W. *J. Am. Chem. Soc.* **2010**, *132* (31), 10668−10670.
(15) Que, L., Jr.; Tolman, W. B. *Nature* **2008**, *455* (7211), 333−340.
(16) Price, J. C.; Barr, E. W.; Tirupati, B.; Bollinger, J. M., Jr.; Krebs, C. *Biochemistry* **2003**, *42* (24), 7497−7508.
(17) Que, L., Jr. *J. Biol. Inorg. Chem.* **2004**, *9* (6), 684−690.
(18) Price, J. C.; Barr, E. W.; Glass, T. E.; Krebs, C.; Bollinger, J. M. *J. Am. Chem. Soc.* **2003**, *125* (43), 13008−13009.
(19) Flashman, E.; Hoffart, L. M.; Hamed, R. B.; Bollinger, J. M.; Krebs, C.; Schofield, C. J. *FEBS J.* **2010**, *277* (19), 4089−4099.
(20) Karlsson, A.; Parales, J. V.; Parales, R. E.; Gibson, D. T.; Eklund, H.; Ramaswamy, S. *Science* **2003**, *299* (5609), 1039−1042.
(21) Krebs, C.; Fujimori, D. G.; Walsh, C. T.; Bollinger, J. M. *Acc. Chem. Res.* **2007**, *40* (7), 484−492.
(22) Punniyamurthy, T.; Velusamy, S.; Iqbal, J. *Chem. Rev.* **2005**, *105* (6), 2329−2363.
(23) Hlavica, P. *Eur. J. Biochem.* **2004**, *271* (22), 4335−4360.
(24) Nam, W. *Acc. Chem. Res.* **2007**, *40* (7), 522−531.
(25) Que, L., Jr. *Acc. Chem. Res.* **2007**, *40* (7), 493−500.
(26) England, J.; Martinho, M.; Farquhar, E. R.; Frisch, J. R.; Bominaar, E. L.; Münck, E.; Que, L., Jr. *Angew. Chem., Int. Ed.* **2009**, *48* (20), 3622−3626.
(27) Rohde, J. U.; In, J. H.; Lim, M. H.; Brennessel, W. W.; Bukowski, M. R.; Stubna, A.; Münck, E.; Nam, W.; Que, L., Jr. *Science* **2003**, *299* (5609), 1037−1039.
(28) Lim, M. H.; Rohde, J. U.; Stubna, A.; Bukowski, M. R.; Costas, M.; Ho, R. Y. N.; Münck, E.; Nam, W.; Que, L., Jr. *Proc. Nat. Acad. Sci. U.S.A.* **2003**, *100* (7), 3665−3670.
(29) Suh, Y.; Seo, M. S.; Kim, K. M.; Kim, Y. S.; Jang, H. G.; Tosha, T.; Kitagawa, T.; Kim, J.; Nam, W. *J. Inorg. Biochem.* **2006**, *100* (4), 627−633.
(30) Grapperhaus, C. A.; Mienert, B.; Bill, E.; Weyhermuller, T.; Wieghardt, K. *Inorg. Chem.* **2000**, *39* (23), 5306−5317.
(31) Kaizer, J.; Klinker, E. J.; Oh, N. Y.; Rohde, J. U.; Song, W. J.; Stubna, A.; Kim, J.; Münck, E.; Nam, W.; Que, L., Jr. *J. Am. Chem. Soc.* **2004**, *126* (2), 472−473.
(32) Fiedler, A. T.; Que, L. J. *Inorg. Chem.* **2009**, *48* (23), 11038−11047.
(33) Rohde, J. U.; In, J. H.; Lim, M. H.; Brennessel, W. W.; Bukowski, M. R.; Stubna, A.; Münck, E.; Nam, W.; Que, L., Jr. *Science* **2003**, *299* (5609), 1037−1039.
(34) Sastri, C. V.; Sook Seo, M.; Joo Park, M.; Mook Kim, K.; Nam, W. *Chem Commun (Cambridge, U.K.)* **2005**, *11*, 1405−1407.
(35) Sastri, C. V.; Park, M. J.; Ohta, T.; Jackson, T. A.; Stubna, A.; Seo, M. S.; Lee, J.; Kim, J.; Kitagawa, T.; Münck, E.; Que, L., Jr.; Nam, W. *J. Am. Chem. Soc.* **2005**, *127* (36), 12494−12495.
(36) Bukowski, M. R.; Comba, P.; Lienke, A.; Limberg, C.; Lopez de Laorden, C.; Merz, M.; Que, L., Jr. *Angew. Chem., Int. Ed.* **2006**, *45* (21), 3446−9.
(37) Bukowski, M. R.; Koehntop, K. D.; Stubna, A.; Bominaar, E. L.; Halfen, J. A.; Münck, E.; Nam, W.; Que, L., Jr. *Science* **2005**, *310* (5750), 1000−1002.
(38) Martinho, M.; Banse, F.; Bartoli, J. F.; Mattioli, T. A.; Battioni, P.; Horner, O.; Bourcier, S.; Girerd, J. J. *Inorg. Chem.* **2005**, *44* (25), 9592−9596.
(39) Balland, V.; Charlot, M. F.; Banse, F.; Girerd, J. J.; Mattioli, T. A.; Bill, E.; Bartoli, J. F.; Battioni, P.; Mansuy, D. *Eur. J. Inorg. Chem.* **2004**, *2*, 301−308.
(40) Pestovsky, O.; Stoian, S.; Bominaar, E. L.; Shan, X. P.; Münck, E.; Que, L., Jr.; Bakac, A. *Angew. Chem., Int. Ed.* **2005**, *44* (42), 6871−6874.
(41) Girerd, J. J.; Banse, F.; Simaan, A. J. *Metal-Oxo and Metal-Peroxo Species in Catalytic Oxidations*; Springer: New York, 2000; Vol. *97*, pp 145−177.
(42) Rohde, J. U.; Bukowski, M. R.; Que, L., Jr. *Curr. Opin. Chem. Biol.* **2003**, *7* (6), 674−682.
(43) Schofield, C. J.; Zhang, Z. *Curr. Opin. Struct. Biol.* **1999**, *9* (6), 722−731.
(44) Liang, H. C.; Dahan, M.; Karlin, K. D. *Curr. Opin. Chem. Biol.* **1999**, *3* (2), 168−175.
(45) Ryle, M. J.; Hausinger, R. P. *Curr. Opin. Chem. Biol.* **2002**, *6* (2), 193−201.
(46) Han, A. R.; Jeong, Y. J.; Kang, Y.; Lee, J. Y.; Seo, M. S.; Nam, W. *Chem. Commun.* **2008**, *9*, 1076−1078.
(47) Nehru, K.; Jang, Y.; Oh, S.; Dallemer, F.; Nam, W.; Kim, J. *Inorg. Chim. Acta* **2008**, *361* (8), 2557−2561.
(48) Lee, Y. M.; Dhuri, S. N.; Sawant, S. C.; Cho, J.; Kubo, M.; Ogura, T.; Fukuzumi, S.; Nam, W. *Angew. Chem., Int. Ed.* **2009**, *48* (10), 1803−1806.
(49) Annaraj, J.; Kim, S.; Seo, M. S.; Lee, Y. M.; Kim, Y.; Kim, S. J.; Choi, Y. S.; Jang, H. G.; Nam, W. *Inorg. Chim. Acta* **2009**, *362* (3), 1031−1034.
(50) Wang, D.; Zhang, M.; Buhlmann, P.; Que, L., Jr. *J. Am. Chem. Soc.* **2010**, *132* (22), 7638−7644.
(51) Mukherjee, A.; Cranswick, M. A.; Chakrabarti, M.; Paine, T. K.; Fujisawa, K.; Münck, E.; Que, L., Jr. *Inorg. Chem.* **2010**, *49* (8), 3618−3628.
(52) Ray, K.; England, J.; Fiedler, A. T.; Martinho, M.; Münck, E.; Que, L., Jr. *Angew. Chem., Int. Ed.* **2008**, *47* (42), 8068−8071.
(53) Yin, G. C. *Coord. Chem. Rev.* **2010**, *254* (15−16), 1826−1842.
(54) White, M. C.; Doyle, A. G.; Jacobsen, E. N. *J. Am. Chem. Soc.* **2001**, *123* (29), 7194−7195.
(55) Ryu, J. Y.; Kim, J.; Costas, M.; Chen, K.; Nam, W.; Que, L., Jr. *Chem. Commun. (Cambridge, U.K.)* **2002**, *12*, 1288−1289.
(56) Mas-Balleste, R.; Que, L., Jr. *J. Am. Chem. Soc.* **2007**, *129* (51), 15964−15972.
(57) Mas-Balleste, R.; Fujita, M.; Que, L., Jr. *Dalton Trans.* **2008**, *14*, 1828−1830.
(58) Rohde, J. U.; Que, L., Jr. *Angew. Chem., Int. Ed.* **2005**, *44* (15), 2255−2258.
(59) Dhuri, S.; Seo, M.; Lee, Y.; Hirao, H.; Wang, Y.; Nam, W.; Shaik, S. *Angew. Chem., Int. Ed.* **2008**, *47* (18), 3356−3359.
(60) Lacy, D. C.; Gupta, R.; Stone, K. L.; Greaves, J.; Ziller, J. W.; Hendrich, M. P.; Borovik, A. S. *J. Am. Chem. Soc.* **2010**, *132* (35), 12188−12190.
(61) Fukuzumi, S.; Kotani, H.; Lee, Y. M.; Nam, W. *J. Am. Chem. Soc.* **2008**, *130* (45), 15134−15142.
(62) Sharma, V. K.; O'Connor, D. B.; Cabelli, D. *Inorg. Chim. Acta* **2004**, *357* (15), 4587−4591.
(63) Makhlynets, O. V.; Das, P.; Taktak, S.; Flook, M.; Mas Ballesté, R.; Rybak Akimova, E. V.; Que, L., Jr. *Chem.—Eur. J.* **2009**, *15* (47), 13171−13180.
(64) Groves, J. T. *J. Inorg. Biochem.* **2006**, *100* (4), 434−447.
(65) Taktak, S.; Ye, W.; Herrera, A. M.; Rybak-Akimova, E. V. *Inorg. Chem.* **2007**, *46* (7), 2929−2942.
(66) Zhdankin, V. V.; Koposov, A. Y.; Litvinov, D. N.; Ferguson, M. J.; McDonald, R.; Luu, T.; Tykwinski, R. R. *J. Org. Chem.* **2005**, *70* (16), 6484−6491.
(67) Hagen, K. S. *Inorg. Chem.* **2000**, *39* (25), 5867−5869.
(68) Sheldrick, G. M. *SHELXTL*, Version 5.04; Siemens Analytical X-ray Insturments: Madison, WI, 1996.
(69) Kent, T. A. *WMOSS; Mössbauer spectral Analysis Software*, v2.5; Minneapolis, 1998.
(70) Evans, D. F. *J. Chem. Soc.* **1959**, *6*, 2003−2005.
(71) Sur, S. K. *J. Magn. Reson.* **1989**, *82* (1), 169−173.
(72) Piguet, C. *J. Chem. Educ.* **1997**, *74* (7), 815−816.
(73) Girerd, J. J. J. Y. In *Physical Methods in Bioinorganic Chemistry*; University Science Books: Sausalito, CA, 2000.
(74) Lane, B. S.; Burgess, K. *Chem. Rev.* **2003**, *103* (7), 2457−2473.
(75) *User Manual of CryoStopped-Flow System*; Hi-Tech Scientific: Bradford on Avon, U.K., 2006.
(76) *To configure and use the Stopped-flow system with J&M Diode array*; Hi-Tech Scientific: Bradford on Avon, U.K., 2008.
(77) *Kinetic Studio, Kinetic Solution for Solution Kinetics*, Version: 1.00; TgK Scientific: Bradford on Avon, U.K., 2008.

(78) Binstead, R. A.; Zuberbühler, A. D.; Jung, B. In *Specfit/32 Global Analysis System*, Version 3.0.36; Spectrum Software Associates: Chapel Hill, NC, 2004.
(79) Karn, J. L.; Busch, D. H. *Inorg. Chem.* **1969**, *8* (5), 1149−1153.
(80) Leugger, A.; Hertli, L.; Kaden, T. A. *Helv. Chim. Acta* **1978**, *61*, 2291−2296.
(81) Drew, M. G. B.; Hollis, S. *Acta Crystallogr., Sect. B: Struct. Sci.* **1980**, *36* (3), 718−720.
(82) Kryatov, S. V.; Mohanraj, B. S.; Tarasov, V. V.; Kryatova, O. P.; Rybak-Akimova, E. V.; Nuthakki, B.; Rusling, J. F.; Staples, R. J.; Nazarenko, A. Y. *Inorg. Chem.* **2002**, *41* (4), 923−930.
(83) Simaan, J.; Poussereau, S.; Blondin, G.; Girerd, J. J.; Defaye, D.; Philouze, C.; Guilhem, J.; Tchertanov, L. *Inorg. Chim. Acta* **2000**, *299* (2), 221−230.
(84) Dewar, R.; Fleischer, E. *Nature* **1969**, *222* (5191), 372−373.
(85) Burns, R. G. In *Mineralogical Applications of Crystal Field Theory*; Cambridge Univ. Press: Cambridge, U.K., 1993.
(86) Greenwood, N. N.; Gibb, T. C. In *Mössbauer Spectroscopy*; Chapman and Hall Ltd.: London, U.K., 1971.
(87) Cranshaw, T. E.; Dale, B. W.; Longworth, D. O.; Johnson, C. E. In *Mössbauer Spectroscopy and its Applications*; Cambridge University Press: Cambridge, U.K., 1985.
(88) Dabrowiak, J. C.; Merrell, P. H.; Stone, J. A.; Busch, D. H. *J. Am. Chem. Soc.* **1973**, *95* (20), 6613−6622.
(89) Shan, X.; Que, L., Jr. *J. Inorg. Biochem.* **2006**, *100* (4), 421−433.
(90) Chen, K.; Costas, M.; Kim, J. H.; Tipton, A. K.; Que, L., Jr. *J. Am. Chem. Soc.* **2002**, *124* (12), 3026−3035.
(91) Jensen, M. P.; Lange, S. J.; Mehn, M. P.; Que, E. L.; Que, L., Jr. *J. Am. Chem. Soc.* **2003**, *125* (8), 2113−2128.
(92) Zang, Y.; Kim, J.; Dong, Y. H.; Wilkinson, E. C.; Appelman, E. H.; Que, L., Jr. *J. Am. Chem. Soc.* **1997**, *119* (18), 4197−4205.
(93) Kim, J.; Zang, Y.; Costas, M.; Harrison, R. G.; Wilkinson, E. C.; Que, L., Jr. *J. Biol. Inorg. Chem.* **2001**, *6* (3), 275−284.
(94) Wada, A.; Ogo, S.; Watanabe, Y.; Mukai, M.; Kitagawa, T.; Jitsukawa, K.; Masuda, H.; Einaga, H. *Inorg. Chem.* **1999**, *38* (16), 3592−3593.
(95) Ogihara, T.; Hikichi, S.; Akita, M.; Uchida, T.; Kitagawa, T.; Moro-oka, Y. *Inorg. Chim. Acta* **2000**, *297* (1−2), 162−170.
(96) Gosiewska, S.; Permentier, H. P.; Bruins, A. P.; van Koten, G.; Gebbink, R. J. M. *Dalton Trans.* **2007**, *31*, 3365−3368.
(97) Jensen, M. P.; Costas, M.; Ho, R. Y. N.; Kaizer, J.; Payeras, A. M. I.; Münck, E.; Que, L., Jr.; Rohde, J. U.; Stubna, A. *J. Am. Chem. Soc.* **2005**, *127* (30), 10512−10525.
(98) Bukowski, M. R.; Halfen, H. L.; van den Berg, T. A.; Halfen, J. A.; Que, L., Jr. *Angew. Chem., Int. Ed.* **2005**, *44* (4), 584−587.
(99) Dabrowiak, J. C.; Merrell, P. H.; Stone, J. A.; Busch, D. H. *J. Am. Chem. Soc.* **1973**, *95* (20), 6613−6622.
(100) Barefield, E. K.; Busch, D. H.; Ochiai, E.; Tokel, N. E.; Lovecchi, F. V. *Inorg. Chem.* **1972**, *11* (2), 283−288.
(101) Geraskin, I. M.; Luedtke, M. W.; Neu, H. M.; Nemykin, V. N.; Zhdankin, V. V. *Tetrahedron Lett.* **2008**, *49* (52), 7410−7412.
(102) Zhdankin, V. V.; Stang, P. J. *Chem. Rev.* **2008**, *108* (12), 5299−5358.
(103) Sharefkin, J. G.; Saltzman, H. *Anal. Chem.* **1963**, *35* (10), 1428−1431.
(104) Geraskin, I. M.; Pavlova, O.; Neu, H. M.; Yusubov, M. S.; Nemykin, V. N.; Zhdankin, V. V. *Adv. Synth. Catal.* **2009**, *351* (5), 733−737.
(105) Decker, A.; Rohde, J. U.; Que, L., Jr.; Solomon, E. I. *J. Am. Chem. Soc.* **2004**, *126* (17), 5378−5379.
(106) Decker, A.; Rohde, J. U.; Klinker, E. J.; Wong, S. D.; Que, L., Jr.; Solomon, E. I. *J. Am. Chem. Soc.* **2007**, *129* (51), 15983−15996.
(107) Gold, A.; Jayaraj, K.; Doppelt, P.; Weiss, R.; Chottard, G.; Bill, E.; Ding, X.; Trautwein, A. X. *J. Am. Chem. Soc.* **1988**, *110* (17), 5756−5761.
(108) Jayaraj, K.; Gold, A.; Austin, R. N.; Ball, L. M.; Terner, J.; Mandon, D.; Weiss, R.; Fischer, J.; DeCian, A.; Bill, E.; Muther, M.; Schunemann, V.; Trautwein, A. X. *Inorg. Chem.* **1997**, *36* (20), 4555−4566.
(109) Costas, M.; Rohde, J. U.; Stubna, A.; Ho, R. Y.; Quaroni, L.; Münck, E.; Que, L., Jr. *J. Am. Chem. Soc.* **2001**, *123* (51), 12931−12932.
(110) Berry, J. F.; Bill, E.; Bothe, E.; Weyhermüller, T.; Wieghardt, K. *J. Am. Chem. Soc.* **2005**, *127* (33), 11550−11551.
(111) Zhou, Y.; Shan, X.; Mas-Balleste, R.; Bukowski, M. R.; Stubna, A.; Chakrabarti, M.; Slominski, L.; Halfen, J. A.; Münck, E.; Que, L., Jr. *Angew. Chem., Int. Ed.* **2008**, *47* (10), 1896−1899.
(112) Park, M. J.; Lee, J.; Suh, Y.; Kim, J.; Nam, W. *J. Am. Chem. Soc.* **2006**, *128* (8), 2630−2634.
(113) de Visser, S. P.; Shaik, S. *J. Am. Chem. Soc.* **2003**, *125* (24), 7413−7424.
(114) de Visser, S. P.; Oh, K.; Han, A. R.; Nam, W. *Inorg. Chem.* **2007**, *46* (11), 4632−4641.
(115) Huang, R.; Espenson, J. H. *J. Mol. Catal. A: Chem.* **2001**, *168* (1−2), 39−46.
(116) Wang, Y.; Espenson, J. H. *Inorg. Chem.* **2002**, *41* (8), 2266−2274.
(117) Wang, Y.; Lente, G.; Espenson, J. H. *Inorg. Chem.* **2002**, *41* (5), 1272−1280.
(118) Kryatov, S. V.; Rybak-Akimova, E. V.; Que, L., Jr. *Abstr. Pap.—Am. Chem. Soc.* **2004**, *228*, 67−74.
(119) Bukowski, M. R.; Comba, P.; Lienke, A.; Limberg, C.; Lopez de Laorden, C.; Mas-Balleste, R.; Merz, M.; Que, L., Jr. *Angew. Chem., Int. Ed.* **2006**, *45* (21), 3446−3449.
(120) Chow, T. W. S.; Wong, E. L. M.; Guo, Z.; Liu, Y. G.; Huang, J. S.; Che, C. M. *J. Am. Chem. Soc.* **2010**, *132* (38), 13229−13239.
(121) Melnyk, A. C.; Kildahl, N. K.; Rendina, A. R.; Busch, D. H. *J. Am. Chem. Soc.* **1979**, *101* (12), 3232−3240.
(122) Busch, D. H.; Farmery, K.; Goedken, V.; Katovic, V.; Melnyk, A. C.; Sperati, C. R.; Tokel, N. *Adv. Chem. Ser.* **1971**, *100*, 44−78.
(123) Cairns, C. J.; Heckman, R. A.; Melnyk, A. C.; Davis, W. M.; Busch, D. H. *J. Chem. Soc., Dalton Trans.* **1987**, *1987* (11), 2505−2510.
(124) Zhang, D. L.; Busch, D. H.; Lennon, P. L.; Weiss, R. H.; Neumann, W. L.; Riley, D. P. *Inorg. Chem.* **1998**, *37* (5), 956−963.
(125) Paschke, J.; Kirsch, M.; Korth, H.; de Groot, H.; Sustmann, R. *J. Am. Chem. Soc.* **2001**, *123* (44), 11099−11100.
(126) Zhang, X.; Zhang, D.; Busch, D. H.; Eldik, R. *J. Chem. Soc., Dalton Trans.* **1999**, *1999* (16), 2751−2758.
(127) Shan, X.; Rohde, J. U.; Koehntop, K. D.; Zhou, Y.; Bukowski, M. R.; Costas, M.; Fujisawa, K.; Que, L., Jr. *Inorg. Chem.* **2007**, *46* (20), 8410−8417.
(128) Kaizer, J.; Costas, M.; Que, L., Jr. *Angew. Chem., Int. Ed.* **2003**, *42* (31), 3671−3673.
(129) Kryatov, S. V.; Rybak-Akimova, E. V.; Schindler, S. *Chem. Rev* **2005**, *105* (6), 2175−2226.
(130) Rybak-Akimova, E. V. Mechanisms of Oxygen Binding and Activation at Transition Metal Centers. In *Physical Inorganic Chemistry*; Bakac, A., Ed.; Wiley: Hoboken, NJ, 1998; Vol. 2, Chapter 4.
(131) Hessenauer-Ilicheva, N.; Franke, A.; Meyer, D.; Woggon, W. D.; van Eldik, R. *J. Am. Chem. Soc.* **2007**, *129* (41), 12473−12479.
(132) Franke, A.; Fertinger, C.; van Eldik, R. *Angew. Chem., Int. Ed.* **2008**, *47* (28), 5238−5242.
(133) Rohde, J. U.; Stubna, A.; Bominaar, E. L.; Münck, E.; Nam, W.; Que, L., Jr. *Inorg. Chem.* **2006**, *45* (16), 6435−6445.
(134) Sastri, C. V.; Lee, J.; Oh, K.; Lee, Y. J.; Jackson, T. A.; Ray, K.; Hirao, H.; Shin, W.; Halfen, J. A.; Kim, J.; Que, L.; Shaik, S.; Nam, W. *Proc. Natl. Acad. Sci. U.S.A.* **2007**, *104* (49), 19181−19186.
(135) Nam, W. W.; Ho, R.; Valentine, J. S. *J. Am. Chem. Soc.* **1991**, *113* (18), 7052−7054.